AN INVESTIGATION OF THE EFFECT OF ENVIRONMENTAL GASES AND PRESSURE ON THE IGNITION OF SOLID ROCKET PROPELLANTS

by

J. D. Hightower

Research Department

ABSTRACT. An investigation was made of the effect of environmental gases and pressures on the ignition of an ammonium perchlorate propellant. In addition, ignition studies were conducted on the individual propellant ingredients. Environmental gases used were air, oxygen, nitrogen, methane and helium. Pressures were 15, 45, and 100 psia. Tests were run in oxygen on an inert mixture of the propellant binder and glass beads and on pressed ammonium perchlorate in methane. Ignition was initiated by radiant energy flux densities over the range of 6.5 to 120 cal/cm^2 sec in an arc-image furnace utilizing a 2,500 watt xenon source. The results indicate that the major exothermic reaction responsible for rapid convergence to steady state deflagration occurs in the gas phase immediately adjacent to the propellant surface.

The shortest ignition times were obtained with oxygen as the environmental gas. The ignition times of both propellant and inert formulation were the same in this environment. Ignition times of the propellant in nitrogen were longer than in oxygen but approximately the same as the ignition time of pressed pellets in methane. The ignition times of the propellant in inert atmosphere was found to increase with decreasing molecular weight of the environmental gas. At the higher flux densities the ignition time was found to be dependent on the environmental pressure with ignition times increasing with decreasing pressure. These results have been discussed in terms of a simple ignition model with (a) no chemical heating, (b) chemical heating in the condensed phase and (c) chemical heating in the gas phase.

NAVAL WEAPONS CENTER

CHINA LAKE, CALIFORNIA ★ OCTOBER 1967

NOV 15 1967

D

106

CLEARINGHOUSE

NAVAL WEAPONS CENTER
AN ACTIVITY OF THE NAVAL MATERIAL COMMAND

M. R. Etheridge, Capt.,USN .... Commander
H. G. Wilson .... Technical Director (Acting)

FOREWORD

This report is a facsimile of the Master of Science thesis en-
titled "An Investigation of the Effect of Environmental Gases and
Pressure on the Ignition of Solid Rocket Propellants" prepared by
J. D. Hightower for the University of California, Los Angeles, Califor-
nia. This program was sponsored by the Naval Ordnance Systems Command.

This report is transmitted for information only. It does not repre-
sent the official view or final judgment of the Naval Weapons Center.

Released by
HUGH W. HUNTER, Head
Research Department
5 October 1967

Under authority of
H. G. WILSON
Technical Director (Acting)

ii

TABLE OF CONTENTS

LIST OF FIGURES

LIST OF TABLES

NOMENCLATURE

Symbol	Definition	Units
B	Preexponential factor	cal/cm^3 sec
c	Specific heat	cal/gm °C
C_R	Rotameter orifice coefficient	dimensionless
D_f	Rotameter float diameter	inches
E	Chemical activation energy	cal/mole
h_{cx}	Local convective heat transfer coefficient	$BTU/hr\ ft^2$°F, cal/cm^2 sec °C
k	Thermal conductivity	cal/cm sec °K
Pr	Prandtl number	dimensionless
$\dot{q}$	Incident flux density	cal/cm^2 sec
$\dot{Q}$	Volumetric flow rate	ml/min
R	Gas constant 1.987	cal/mole °K
R	Rotameter diameter ratio	dimensionless
Re	Reynolds number	dimensionless
t	Time	sec, msec
T_i	Ignition time	sec, msec
T_s	Surface temperature	°K
T_o	Initial temperature	°K
W_f	Weight of rotameter float	gm
x	Space-distance variable	in, cm
α	$\dfrac{k}{\rho c}$ = thermal diffusivity	cm^2/sec

Symbol

ΔT_s	$T-T_o$	°K
μ	Absolute viscosity	gm/cm sec
π	Numerical constant (3.14159)	dimensionless
ρ	density	gm/cc

INTRODUCTION

The successful operation of a solid propellant rocket encompasses a broad spectrum of scientific and engineering disiplines ranging from the fundamental laws of motion to the extreme complexities of solid propellant combustion processes. The rocket performance, per se, is initiated with the ignition transient which includes the thermal ignition of the propellant surface in the vicinity of the igniter, flame spreading over the entire exposed surface area, and the chamber filling and pressure rise which leads to the final steady state motor operating conditions. In the early days of modern rocketry little attention was given to fundamental mechanisms of propellant ignition. Instead, rules of thumb and empirical correlations were used which led to the development of the "art" of ignition system design.

Even now the design of ignition systems is largely empirical and design progress has kept pace with new propulsion concepts and demands through extensive igniter development programs. The demands of space age requirements for larger, more advanced propulsive systems, often employing exotic fuels and operating under adverse environmental conditions, have made it imperative to predict motor ignition behavior with a minimum of expensive testing. This in turn has made it necessary to study the basic mechanisms that control the solid propellant ignition processes. The general goal of such work is to evolve a body of knowledge which will enable rational design of ignition systems.

1

Considerable work in recent years has been devoted to the study of solid propellant ignition processes and various theories have been advanced to explain observed ignition behavior. Briefly, it has been variously proposed that the controlling mechanisms in the ignition transient leading to steady state deflagration occur in the condensed phase, in the gas phase, or at the gas-solid interface. The fact that solid propellants are often very complex, both chemically and physically, allows for the possibility that any of these proposed mechanisms may dominate ignition. Additionally, all of the proposed mechanisms may contribute significantly to the ignition process in different regions over the total range of interest.

A comprehensive study of rocket motor ignition systems would include not only a mechanistic explanation of the observed response of the surface ignition of a propellant to a particular type of external energy stimulus but also the effect of a combination of the different modes that may be supplied by a rocket igniter. This should include various combinations of (1) convective heating from hot gases, (2) conductive heating from hot particles impinging or condensing on the surface, (3) radiation from hot gases and incandescent particles, or (4) hypergolic heating from highly reactive chemical species. Information of this type, in addition to a knowledge of the rate of flame spread over the grain surface and the rate chamber pressurization, would aid the rocket engineer in designing a predictable ignition system.

The present work may be regarded as a contribution to such a study. The emphasis has been placed on a specific study of the ignition of an ammonium perchlorate (AP) composite propellant to obtain a better

understanding of the ignition process. The objectives of the work

described in this thesis are:

1. To develop experimental arc-image furnace equipment and

   techniques for the purpose of improving the accuracy and

   ease of obtaining solid propellant ignition data.

2. To investigate the initiation of ignition of a typical

   ammonium perchlorate based composite propellant, and the

   individual propellant ingredients, by high intensity thermal

   radiation in an arc image furnace.

3. To determine, experimentally, significant chemical reactions

   or dominant processes that are important to the ignition

   mechanism.

4. To study the effect on ignition of (a) the type of environ-

   mental gas, (b) the pressure of the environmental gas, and

   (c) the magnitude of the externally applied eat flux.

The overall objective of this work has been to distinguish

between proposed mechanisms that may dominate the ignition process

when high intensity thermal radiation is used as the external energy

stimulus. Future work will be required to define the relationship

between coupled modes of heat transfer on the ignition characteristics

of solid propellants. It is hoped that these data will be useful as

future guidelines in formulating an improveu model of the ignition

process.

IGNITION THEORIES

A solid propellant is defined as being ignited when chemical and thermal activity at or near the surface is in such a state that rapid and spontaneous convergence to steady-state burning occurs. Because of the complexity of composite solid propellants there are many possibilities for combustion and ignition reactions. The complexity of the process is such that none of the current theories include all possible reactions and energy feedback to the propellant surface. The present analytical models of ignition have evolved primarily as attempts to explain the effect of environmental factors on the observed ignition behavior of propellants. Of necessity, each of the theories has to some degree over-simplified the physical characteristics of the system under study. Additionally, each of the models has assumed a completely different external energy stimulus making any valid comparison between models difficult if not impossible. A current comprehensive review of ignition theories has been published by Price and co-workers [59].

CONDENSED PHASE IGNITION THEORY

The condensed phase theory is based on the assumption that the ignition process is controlled by the temperature of the solid phase. In its simplest form the condensed phase theory does not consider a chemical heating term but assumes that the propellant undergoes precipitous ignition at an invariant surface temperature. This concept was employed by Altman and Grant [2] who studied the ignition of composite propellants by heating the propellant with embedded electrical heating wires.

4

Hicks [34] carried out a numerical analysis of a "surface ig-
nition" model which considered transient heating analysis with exo-
thermic chemical heating in the solid. This exothermic self-heating in
the solid was assumed to follow the Arrhenius rate equation with an
exponential dependency on temperature. In his analysis Hicks also con-
sidered the thermal transient that resulted upon removal of external
heating. Hicks' theory was evolved at a time when most propellants
were of the double-base type. Since then other investigators have con-
sidered the condensed phase model in connection with composite propel-
lants. Baer and Ryan [8, 9, 10], Evans, Beyer and McCulley [23],
Keller [39], and Price, et al [60] have considered solid phase models
with different assumptions regarding external heating and self-heating.
Price, et al, in their recent review [59] have considered solid
phase model in detail.

GAS PHASE THEORY

Observations by Summerfield and McAlevy [66] of the ignition of
ammonium perchlorate composite propellants in a shock tube filled with
a nitrogen-oxygen environmental gas led McAlevy, Cowan and Summerfield
[49] to develop the gas-phase theory of propellant ignition. This
theory assumes that the fuel binder decomposes and diffuses into the
hot oxidizing gas where eventual vigorous exothermic reactions occur
supplying the necessary energy feedback to the surface for rapid
attainment of steady-state burning. The rate controlling reactions are
presumed to be those occurring in the gas phase near the vaporizing
surface. The ignition time is assumed to be the time required for
sufficient fuel to vaporize and reach a suitable concentration for a

5

combustible gas mixture. Heating of the surface is assumed to occur
with a step rise in surface temperature and concurrent decomposition of
the fuel. The criterion for ignition is for chemical heat generation
in the gas phase to be equal to local heat losses. Experimentally ob-
served ignition times were not correlated well by the theory. In a
subsequent publication [67] it was indicated that the original corre-
lation between theory and experiment was not conclusive because of data
scatter. More recent work on this model has been done by Hermance,
et al [33].

HETEROGENEOUS THEORY

Ignition that results from significant reactions between the
propellant surface and the environment gas, between the propellant in-
gredients or between the decomposition products of a particular ingre-
dient and the condensed phase of the other ingredient, is termed
"heterogeneous ignition". Allen and Pinns [1] studied the ignition of
propellants and propellant ingredients by gaseous chlorine trifluoride
at room temperature and showed that spontaneous ignition would occur.
These results suggested the possibility that weaker oxidizing gases
could be important at higher temperatures such as those present during
ignition by external heating. Anderson, et al [ ] studied the effect
of oxidizer fraction and pressure of the environmental gas on ignition
of binders and propellants with fluorine and chlorine trifluoride and
developed a hypergolic ignition theory to permit calculation of ig-
nition delay times. In a qualitative extension of the hypergolic
theory it is suggested [5] that the rate controlling reactions in the
ignition of composite propellants are spontaneous heterogeneous

6

reactions between decomposition products of the solid oxidizer and the binder fuel. The "heterogeneous theory", at present, remains qualitative in nature.

THE CRITERION OF IGNITION

The attainment of a condition of steady state deflagration of a solid propellant commences with the application of an external energy stimulus, which serves to raise the temperature of the propellant to a state of affairs where chemical heating becomes dominant, and culminates in the final precipitous temperature rise to steady state values. In the models that have been described above, provision is not made to include the final steady state condition and the definition of ignition is somewhat arbitrary with the exact choice being determined for mathematical convenience. These definitions include such choices as a predetermined surface temperature rise rate (in the range of 10^6 °C/sec), the behavior of the surface temperature following removal of the external heating stimulus (here the onset of surface temperature increase in some specified time following removal of the stimulus would be taken as an indication of ignition) with ignition "time" being the period of external heating, or finally a state of "ignitedness" is assumed when the rate of chemical heat generation at or near the surface is just greater than the energy losses from the system.

From a practical viewpoint, the problem of definition of attainment of ignition is alleviated by the fact that the chemical heating processes are exponentially rate dependent on temperature with the result that "runaway" conditions are achieved in a very short interval after any time when the chemical heating has become appreciable.

7

Thus, almost all experimental techniques for detecting ignition would then yield nearly the same results. It is possible of course to find conditions where different methods of ignition detection would give different results under the same experimental conditions. These issues have been belabored at length by various investigators and it seems unlikely that universal acceptance of a particular method will be forthcoming in the immediate future. It is not the intent of the present work to resolve this issue. Within the framework of the type of ignition experiment performed here, a reasonable criterion of ignition was assumed to be the onset of detectable self-luminosity from exothermic reactions at or very near the propellant surface. This serves to define ignition as used subsequently in this work.

DESCRIPTION OF THE EXPERIMENT

The goal of solid propellant ignition research is to obtain a better understanding of the fundamental mechanisms involved in the ignition transient by observing ignition behavior under carefully controlled test conditions. The general method of approach for experimental ignition research is to expose a propellant sample, in a carefully controlled environment, to an external energy stimulus of known but adjustable magnitude, and observe the time necessary for ignition to occur. The arc-image furnace is an excellent laboratory tool for obtaining precise test conditions for ignition research. The image furnace is an optical system designed to focus and concentrate radiant energy from a suitable source onto a sample target. The use of image furnaces for the concentration of radiant energy dates from ancient times and several papers have been published on their history, general characteristics and use as a research tool [29, 35, 56].

There are several advantages offered by the image furnace over other sources of thermal energy:

1. The energy is supplied in a "clean" form in that it is independent of the test sample environment.

2. The behavior of the sample can be studied in a controlled environment over a wide range of pressure.

3. The sample can be exposed to the full intensity of the radiant energy very rapidly, and terminated without disturbing the other environmental factors.

4. The energy flux density is easily controlled and reproduced over a wide range.

5. The use of a transparent test cell allows for continuous viewing of the sample throughout the test.

The arc-image furnace, when used for ignition of solid propellants, supplies the external energy stimulus to the propellant surface in the form of high intensity thermal radiation. In order to obtain quantitative ignition data from an arc-image experiment, careful consideration must be given to the instrumentation and associated controls for the measurement and regulation of the incident energy. Attention must also be given to the nature of the energy source in the event that it is unsteady in magnitude such that ignition behavior is significantly affected. In the following sections a discussion of the techniques and associated instrumentation used in this work is presented.

The experimental work for this thesis was performed in the thermal radiation facility located in the Aerothermochemistry Group's laboratory at the U. S. Naval Ordnance Test Station, China Lake, California. The facility consists of an arc image furnace and the necessary equipment and instrumentation for the measurement and control of high intensity thermal radiation. The arc image furnace used in this work basically consists of two opposing ellipsoidal mirrors on a common optical axis with the secondary focal point of each mirror being coincident midway between the mirrors. A high intensity thermal radiation source is located at the primary focus of the first mirror with the test sample being placed at the primary focus of the second mirror. A high speed shutter is located at the coincident second focal point

to control the irradiance-time history of the sample. This arrangement is shown schematically in Fig. 1, and is similar to other facilities that have been described elsewhere [12, 14, 46, 56].

In the present case, thermal radiation supplied by a xenon arc is collected by the primary and auxiliary mirrors and projected to the second focal point (often called the crossover point) where the high speed shutter controls the energy beam and sample exposure in a nearly stepwise fashion. From this coincident second focal point the beam diverges and is collected by a second mirror, similar to the primary mirror, and refocused on the test sample. The sample is located inside a stainless steel chamber fitted with a quartz window to transmit the radiant energy and a photodiode to detect ignition of the sample. The energy beam passes through the window and impinges on a plain circular end of the sample with the maximum flux density at the center. The system is capable of producing a flux density of 120 cal/cm^2 sec inside the chamber with the xenon lamp operating at 80 amps. Different environmental gases at pressures up to 100 psia flow through a well defined rectangular channel between the quartz window and the exposed sample end.

The flux density at the sample position is measured with a commercial radiometer similar to that devised by Gardon [27]. The level of intensity of the flux is controlled by inserting various numbers of wire mesh screen layers in the energy beam. The source is run at a constant energy output. Exposure of the sample is accomplished with a high speed shutter located at the coincident second focus. Flux densities over the range of 6 to 120 cal/cm^2 sec have been used in the present work.
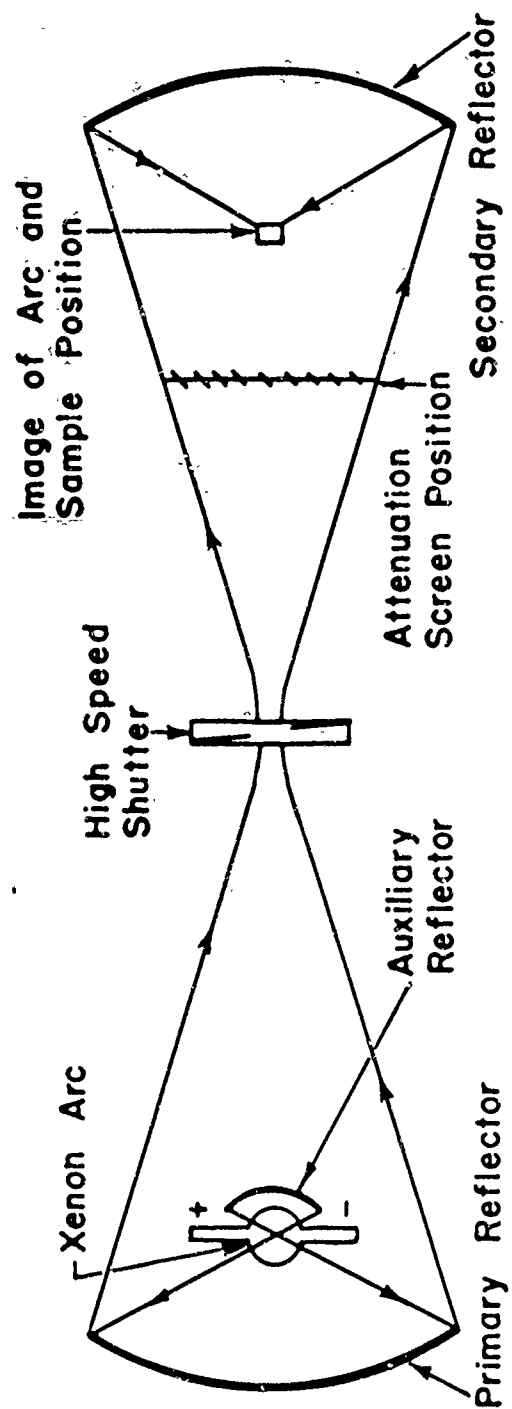
11

FIGURE 1. SCHEMATIC REPRESENTATION OF XENON ARC, ELLIPSOIDAL MIRROR SYSTEM ARC IMAGE FURNACE SHOWING RELATIVE LOCATIONS OF MAJOR COMPONENTS.

Measurement of the expos   time commences with the development

of the maximum flux density, u..   he prevailing test conditions, on

the center of the sample. With the shutter used in the present work

the maximum flux density has been found to occur over a spot 0.030

inches in diameter in 1 millisecond from the initial shutter opening.

Ignition is detected by a photodiode whose optical axis is aligned

parallel with and slightly above the sample surface. The photodiode

then "sees" the sample surface at a low grazing angle and the gas phase

up to approximately 0.15 inches immediately above the center of the

sample. The photodiode also detects scattered background radiation as

well as the propellant ignition. This background radiation allows the

shutter opening to be displayed on the oscilloscope for the beginning

of exposure time. Figure 2 is a sketch of the type of ignition trace

obtained in the present work showing the technique employed in measuring

ignition time. Actual ignition traces photographed from the oscillo-

scope are shown in the appendix in Fig. 25.

The sequence of events constituting a typical ignition test are

as follows:

1. The lamp arc is struck and allowed to come to steady oper-
   ating conditions at 80 amps (approximately 5 minutes).

2. A calibration of the flux density is made with the radiometer.

3. The radiometer is removed from the ignition bomb and the
   sample holder with a freshly prepared sample is mounted in
   the bomb.

4. The environmental gas is admitted to the bomb and the flow
   and pressure is adjusted to the desired level.
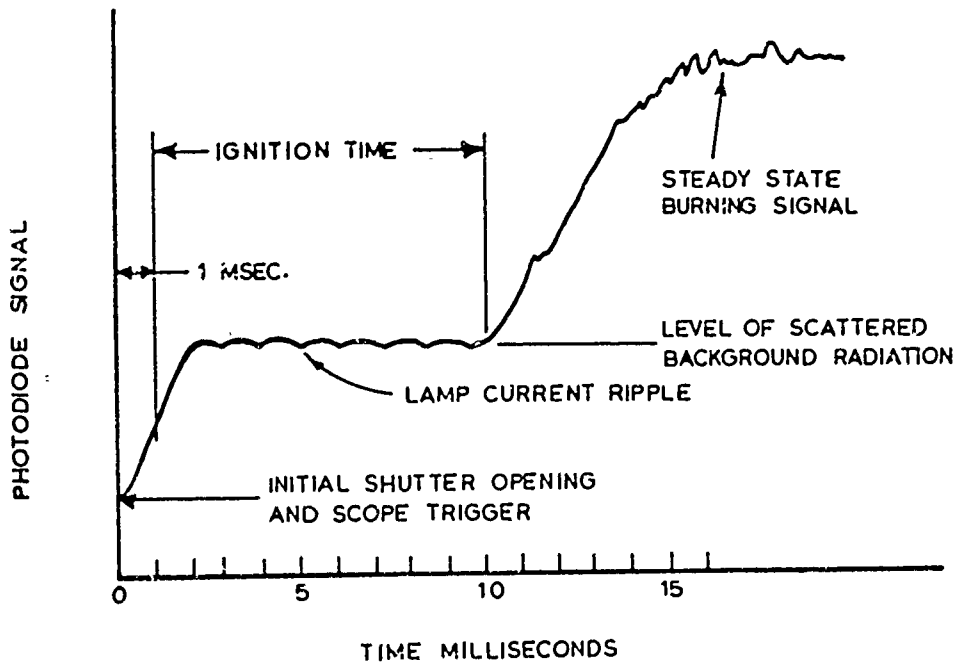
FIGURE 2. SKETCH OF REPRESENTATIVE RADIATION-IGNITION TRACE ILLUSTRATING THE METHOD USED TO MEASURE IGNITION TIME. THIS SKETCH IS TYPICAL OF A HIGH-FLUX, HIGH-PRESSURE TEST. ACTUAL IGNITION TEST TRACES ARE SHOWN IN APPENDIX A, FIG. 25.

5. The main lamphouse dowser is opened which automatically opens the shutter and triggers the oscilloscope. The lamp current meter is monitored visually during the run. In the event that flux variations greater than ± 1 amp occur during the run, the run is rejected.

6. Following ignition the dowser is closed, the gas flow terminated and the bomb is flushed with nitrogen.

7. The ignition time is recorded on the data sheet and the memoscope erased and reset.

This general sequence of events is repeated for five consecutive runs. Following the fifth run a flux calibration is made and the test conditions are varied for the next five runs. This is continued until the

14

ignition response for the propellant is complete over the range of variables of interest.

Ignition tests were run on a typical ammonium perchlorate composite propellant and on the different propellant ingredients. The propellant designated as A-87 in the Aerothermochemistry Division's propellant series contained 75 percent AP, 23.5 percent PBAN (polybutadiene acrylic acid acrylonitrile) binder, 1 percent copper chromite (CC) and 0.5 percent carbon (C). An inert propellant was prepared by substituting glass beads for AP on an equal volumetric basis with the other constituants remaining the same. Ammonium perchlorate pressed pellets, with an AP/CC/C ratio equal to that in the propellant, were prepared by pressing in a cylindrical mold at 40,000 psi. The experimental results and a discussion of their interpretation are presented in the following chapter.

EXPERIMENTAL RESULTS AND DISCUSSION

The general dependence of ignition time of A-87 propellant on the incident flux density is shown in Fig. 3. In this figure the independent parameter is the type of environmental gas at a constant pressure of 45 psia. The most obvious characteristic of the data is that the ignition time decreases with increasing flux density. Further, at a constant value of $\dot{q}$ the ignition time increases with decreasing molecular weight of the environmental gas. The general trend of decreasing ignition time with increasing flux density is common to the other experimental methods of supplying external energy, i.e., conductive or convective.

Before considering the experimental results in detail, it is instructive to consider two simple thermal models of ignition: (1) the case where the propellant is considered as a one-dimensional, semi-infinite, inert solid with ignition occurring at a constant surface temperature, and (2) the same general model, only with a chemical heating term. In both cases, a constant surface heat flux is assumed in conformity with the conditions of the arc image experiment.

Then for case (1) we have

$$\rho c \, \frac{\partial T}{\partial t} = k \, \frac{\partial^2 T}{\partial x^2} \qquad (1)$$
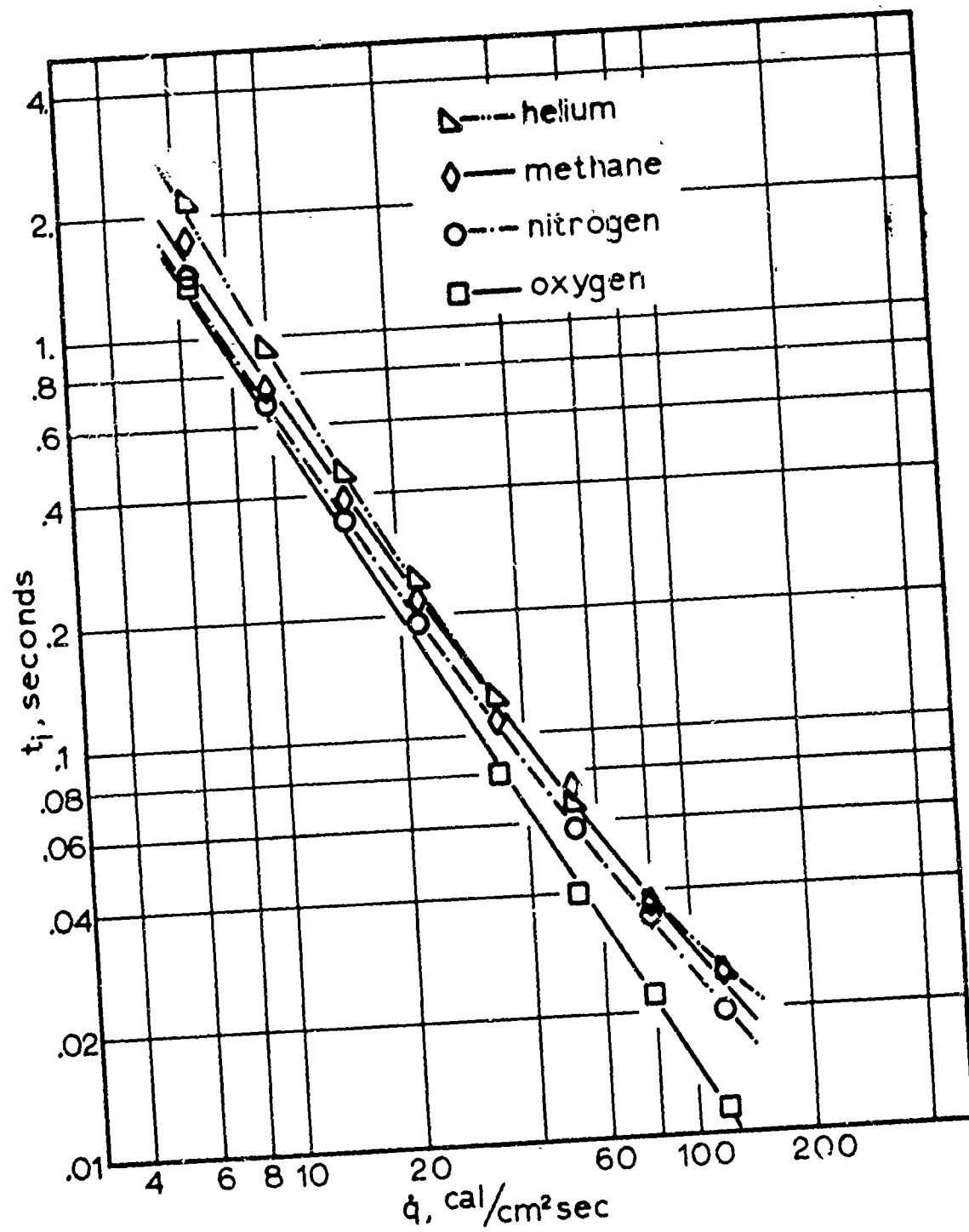
with boundary and initial conditions

16

FIGURE 3.   IGNITION DATA FOR A-87 PROPELLANT IN VARIOUS
ENVIRONMENTAL GASES AT A CONSTANT PRESSURE OF 45 PSIA.

$$-k \frac{\partial T}{\partial x} = \dot{q} \text{ at } x = 0$$

$$\frac{\partial T}{\partial x} = 0 \text{ at } x = \infty$$

$$T = T_o \text{ at } t = 0$$

The well known solution to equation (1) is*

$$T_s - T_o = \frac{2\dot{q}}{k} \left(\frac{\alpha t}{\pi}\right)^{\frac{1}{2}} \qquad (2)$$

If we consider the concept of an invariant autoignition temperature, then we find t_i related to $\dot{q}$ by

$$t_i = C/\dot{q}^2 \qquad (3)$$

and a plot of $\ln t_i$ vs. $\ln \dot{q}^2$ should then yield a straight line with a slope of -2.0.

For case (2) with provision of chemical heating, we have for the one-dimensional heat balance equation

$$\rho C \frac{\partial T}{\partial t} = k \frac{\partial^2 T}{\partial x^2} + B e^{-E/RT} \qquad (4)$$

with the same initial and boundary conditions as (1). Solutions to

---

*See for example Carslaw and Jaeger, <u>Conduction of Heat in Solids</u>, 2nd edition, Oxford at the Clarenden Press, 1959, p. 75.

18

equation (4) have been given [60] for the following values of kinetic parameters

$$B = 10^{19}, \ 10^{22}, \ 10^{25} \ cal/cm^3$$

$$E/R = 15,000, \ 20,000, \ 25,000, \ 30,000°K$$

over a range of flux density from $\dot{q} = 0.01$ to $1,000 \ cal/cm^2$ sec.

The results shown in Fig. 3 indicate that the concept of a constant surface temperature at ignition is not obeyed. The oxygen curve, for example, displays a slope of -1.62. The ignition curves for other environmental gases have slopes somewhat less than this. The only exception is the helium curve at low fluxes which gives a slope of magnitude slightly greater than -1.62. The point of this exercise is simply to indicate that the data are not correlated by a simple heating model with ignition occurring at a constant temperature. In fact, the ignition data shown in Figs. 6, 7, 8, 9 and 10 for the various environmental gases with pressure as the independent parameter all indicate a dependence of ignition time on environmental pressure. This pressure dependence can hardly be explained by such a simple concept.

In case (2) the inclusion of a chemical heating term has moved us closer to the realistic ignition situation where eventual chemical heating must occur. Even though case (2) considers the self-heating to occur only in the condensed phase an examination of the effect of such chemical heating will provide insight into the effect of other modes of heat generation and energy feedback to the propellant surface.

Figures 4 and 5 are similar to those given in reference [60] for the solution to equation (4) for typical values of the kinetic
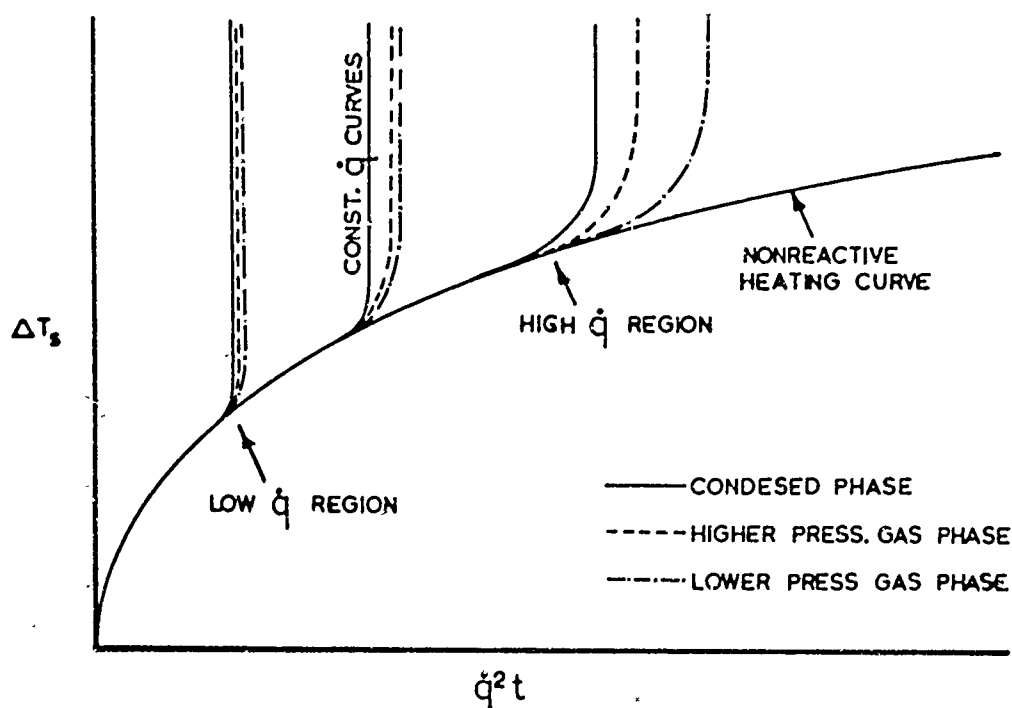
FIGURE 4. TYPICAL CORRELATION OF CALCULATED SURFACE TEMPERATURE RISE AS A FUNCTION OF $\dot{q}^2 t$ AND $\dot{q}$. SOLID $\dot{q}$ CURVES ARE FOR SELF-HEATING IN THE CONDENSED PHASE WITH THE DASHED $\dot{q}$ CURVES REPRESENTING SELF-HEATING IN THE GAS PHASE.

parameters. In Fig. 4 the increase in surface temperature is shown as a function of $\dot{q}^2 t$. The lower curve is the solution for the no-chemical-heating situation. The curves that break away at various values of $\dot{q}$ indicate that the values of surface temperature at which runaway chemical heating occurs is increased at the higher heating rates. The solid curves which break away are representative of the solution of equation (4) with condensed phase chemical heating. The dashed lines correspond to a situation where the first reaction is a decomposition of the propellant ingredients (or a single ingredient) followed by an exothermic reaction in the gas phase.

In the case of condensed phase reactions, the energy feedback coupling mechanism is very efficient, i.e., it is "built into" the
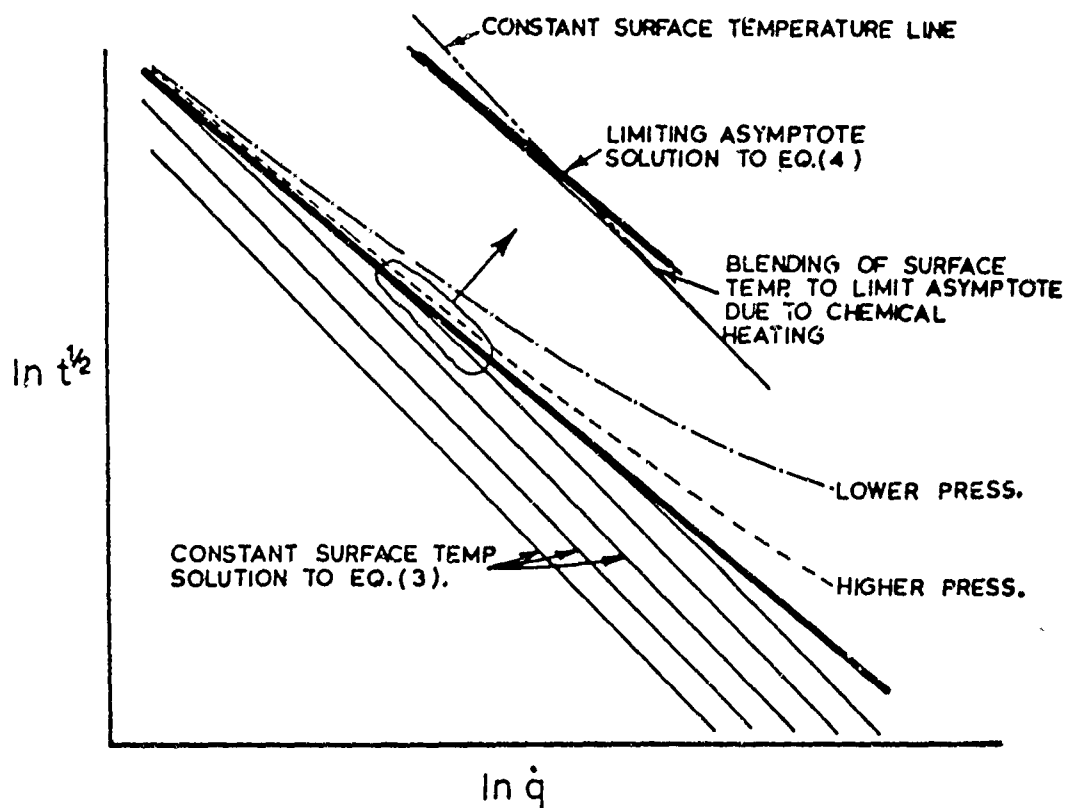
FIGURE 5. SURFACE TEMPERATURE SOLUTIONS OF A SEMI-INFINITE, ONE-DIMENSIONAL SLAB EXPOSED TO A CONSTANT EXTERNAL SURFACE HEAT FLUX WITH AND WITHOUT SELF-HEATING.

propellant surface. As a consequence, when a temperature is reached where chemical heating becomes appreciable, only a very short additional period of time is necessary for the exponential nature of the temperature dependence to produce a precipitous temperature rise and "ignition" has occurred. In the case of a gas phase-controlling exothermic reaction (the dashed lines) the reaction rate will be sensitive to the concentration of the reactable species and hence to gaseous diffusion processes. In the gas phase models that have been developed [32, 49] the dependence on diffusion is strong. Even though these models do not assume a constant external heat flux it is not expected that such a boundary condition would alter this dependence.

21

Figure 5 is a cross plot of Fig. 4 with the ordinate and abscissa being those used to correlate the present experimental data. The dark solid line represents an upper asymptote for the near vertical section of the condensed phase constant $\dot{q}$ curves that break away from the no-chemical-heating curve of Fig. 4. The extremely narrow spacing of the constant surface temperature lines ($\rightarrow 1/\infty$) near the limiting asymptote reflects the precipitous departure of the constant $\dot{q}$ lines from the inert heating situation. Here we see that the inclusion of chemical heating in the heat balance equation leads to a limiting asymptote with the result that the constant temperature surface lines become greatly compressed in the region very close to this limit. The slope of this limit asymptote in magnitude is less than -1 indicating that with chemical heating we do not obtain a constant ignition temperature.

The dashed lines in Fig. 5 representing "higher" and "lower" pressure correspond to the dashed curves of constant $\dot{q}$ in Fig. 4 for a gas phase, exothermic reaction. In this case the effect of gaseous diffusion (increasing for decreasing pressure and/or molecular weight) is to delay the accumulation of reactable species in sufficient concentration to produce an appreciable exothermic reaction. In addition, the coupling of the chemical heating energy to the surface is less efficient than for the condensed phase, since it is by conduction in the gas phase. Also, on a relative time scale, the variation of precipitous temperature rise of the condensed phase curves, compared with gas phase curves of Fig. 4, is greater at high flux than at low flux. This is indicated in Fig. 5 where it can be seen that the higher and

lower pressure curves merge together and approach the limiting asymptote curve for condensed phase chemical heating at lower flux values. In the low flux region, then, ignition data plotted as $\ln t_i^{\frac{1}{2}}$ vs. $\ln \dot{q}$ would appear to be well correlated by a simple condensed phase model such as that described by equation (4).

The concept of a one-dimensional, semi-infinite, inert slab heated at a constant rate is useful in estimating the general range of surface temperatures that prevail at ignition. Sample calculations for air at 45 psia (using equation (3)) indicate that the surface temperature at ignition at an incident flux of 6.45 cal/cm^2 sec is on the order of 330°C and at 120 cal/cm^2 sec is on the order of 775°C. The values thus calculated are only approximations and at the higher heating rate the value is no doubt in greater error due to evaporation, sublimation and other heat losses unaccounted for in the computations. It is interesting, however, that the ignition temperatures at low fluxes approach those at which the first rapid decomposition of ammonium perchlorate begins in a differential thermal analysis.* This rapid decomposition temperature tends to shift to higher temperatures as the differential thermal analysis heating rate is increased.

It is now of interest to examine the data of the present work in light of the ignition model discussed above. The ignition data of A-87 is shown in Figs. 6, 7, 8, 9, 10 and 11 with Fig. 8 showing the dependence of A-87 ignition on oxygen concentration at the highest flux level. Figures 12 and 13 show the ignition data of the dummy propellant

---

*Private communication with Dr. K. Kraeutle, U. S. Naval Ordnance Test Test Station, China Lake, California, January, 1967.

and pressed pellets respectively. Tabulation of the experimental data is given in Appendix D.

First, let us consider the ignition data of A-87. It is observed that all of the data have a slope of less than -1. All of the data display a pressure dependence, with the relative difficulty of ignition increasing with decreasing pressure at high flux. At low flux the pressure dependence tends to reverse itself with the high pressure data displaying slightly longer ignition times than the low pressure data. With the ignition detection system used, it was not possible to obtain data at 15 psia at the higher flux levels when any of the gases, except air or oxygen, were used. The trend of the data for low pressure indicates that inert gases would also display a strong pressure dependence if the detection system were sensitive enough to obtain data in this region.

Figure 6 shows the data of A-87 ignition in air. With air as the environmental gas, it was possible to run tests at 15 psia at the highest flux and obtain a weak but definite ignition signal. The presence of 20 percent oxygen then, considerably increased the rate of the reaction "seen" by the photodiode. The pure oxygen data are shown in Fig. 7. All ignition signals were strong with pure oxygen indicating a still greater increase in reaction rate as would be expected. A strong pressure dependence is observed with air at high fluxes while oxygen displayed the least pressure dependence of any of the gases (assuming the extrapolated trends of low pressure - high flux data of inert gases are essentially correct). Figure 8 is a plot of ln t_i vs. ln oxygen concentration for the air and oxygen data at the
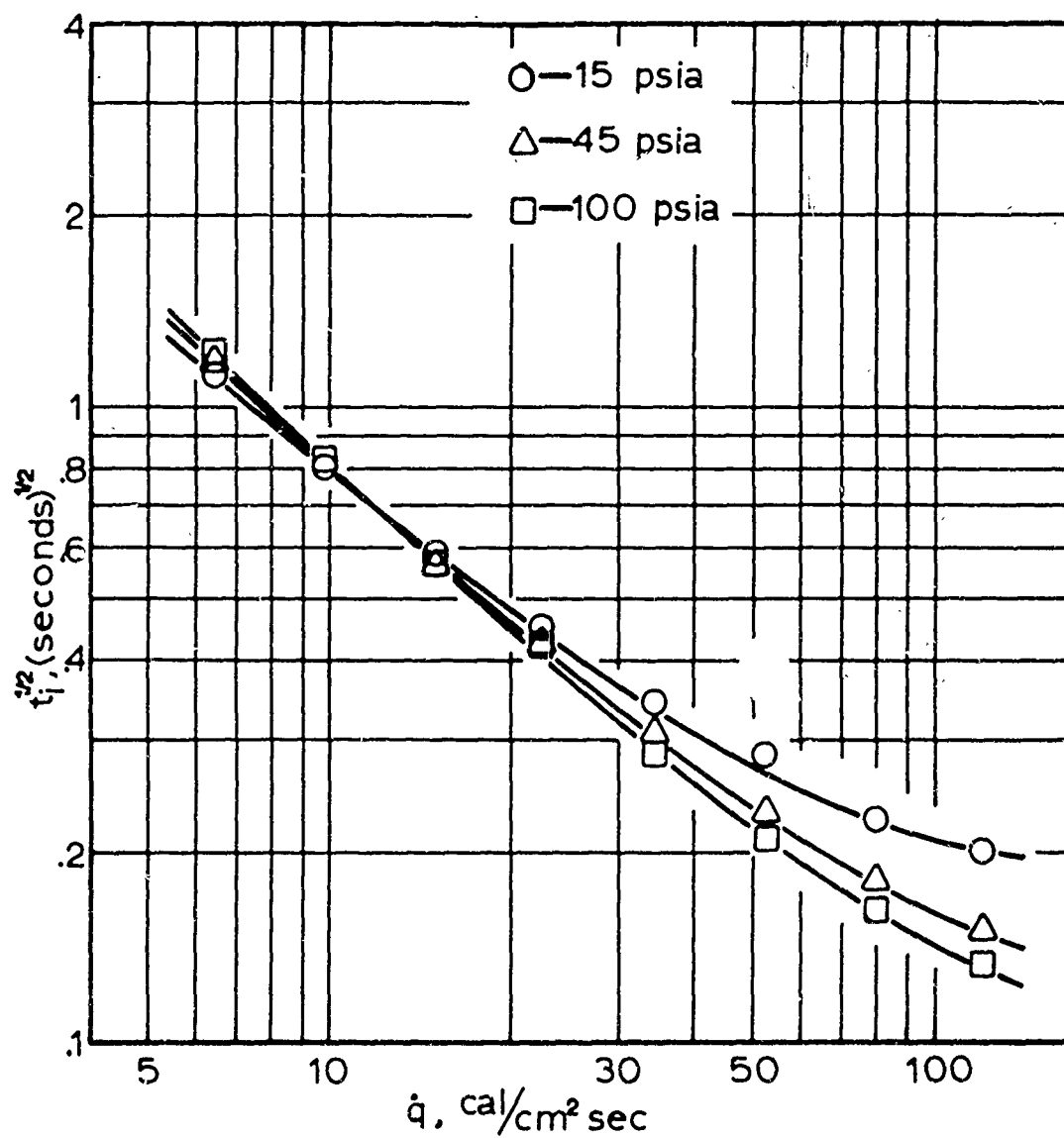
FIGURE 6.   IGNITION DATA FOR A-87 PROPELLANT IN
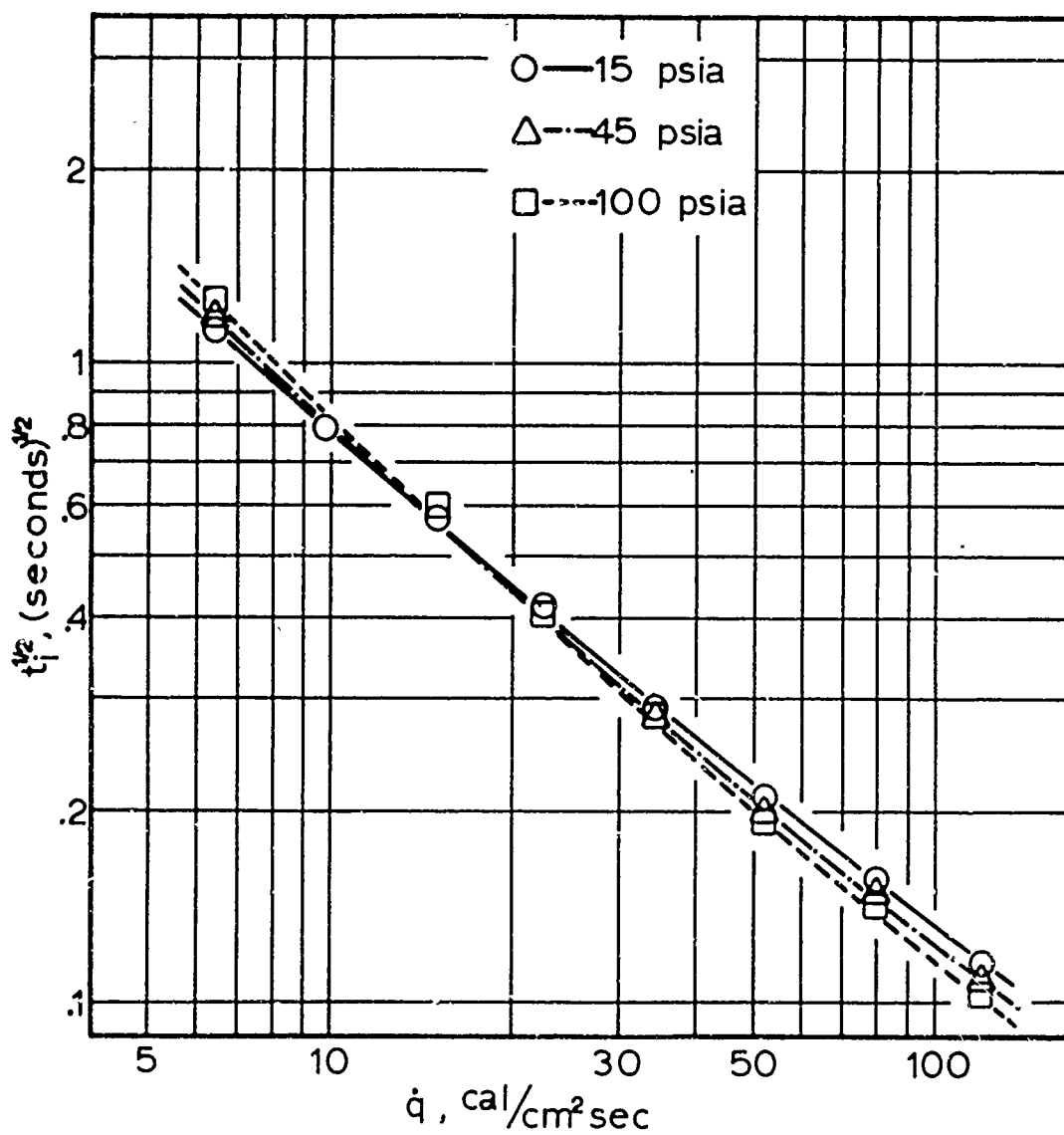AIR AT TEST-GAS PRESSURES OF 15, 45 AND 100 PSIA.

FIGURE 7. IGNITION DATA FOR A-87 PROPELLANT IN OXYGEN
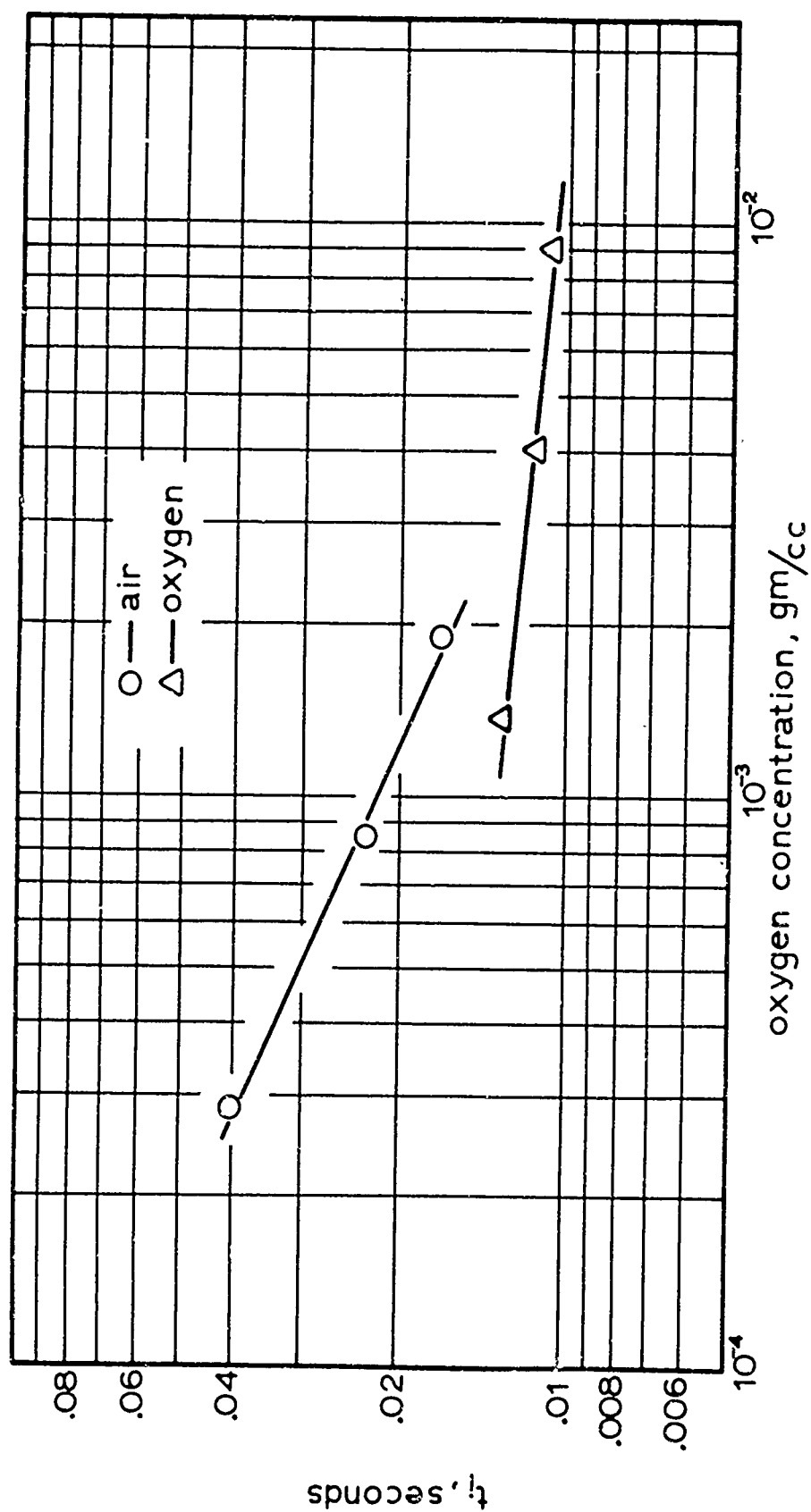AT TEST-GAS PRESSURES OF 15, 45 AND 100 PSIA.

FIGURE 8. IGNITION DATA FOR A-87 PROPELLANT
IN AIR AND OXYGEN AT 120 CAL/CM² SEC.

highest flux level. These data indicate that for oxygen-containing gases the dependence of ignition time on oxygen concentration is differ, if the concentration is varied by mole fraction or total pressure. This suggests a diffusion limited reaction, i.e., the reaction kinetics are fast enough to consume the oxygen as fast as it can be supplied. In the case of air the ignition time dependence is increased due to the presence of nitrogen impeding the diffusion of oxygen.

When considering the data in inert gases (Figs. 9, 10 and 11), it must be remembered that we now have to rely on both propellant ingredients to commence decomposition at a rate that is sufficient to supply both reactants in the necessary concentration to allow ignition to occur under the prevailing conditions of temperature and pressure. Here, we expect to find the effect of diffusivity of the environmental gas to be important. Gases with high diffusivity are able to effectively dilute the concentration of reactable species during the initial decomposition stages and, hence, we have to wait longer for the accumulation of reactants and for the surface temperature to increase, to provide an increased rate of decomposition.

We can expect this effect to be stronger at lower pressures where diffusion of reactive species away from the surface and diluent species to the surface would be enhanced. Unfortunately, it was not possible to obtain reliable data at low pressure and high flux where this effect would be most pronounced. The data trends are in the right direction, however, and comparison of the data of different gases at the same pressure (Fig. 3) indicates the importance of the diffusional effect. Further, the lack of strong pressure dependence with pure
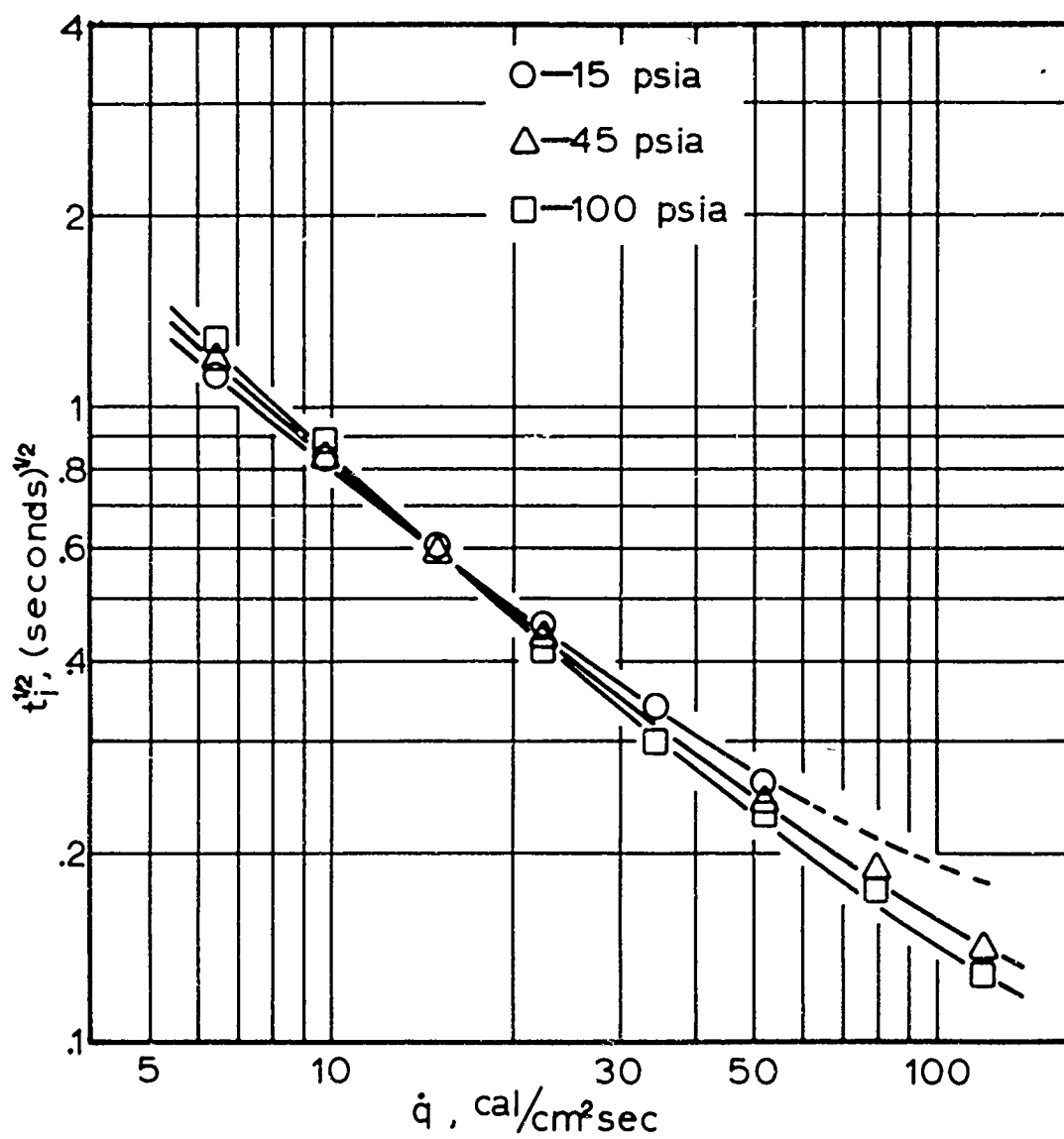
FIGURE 9. IGNITION DATA FOR A-87 PROPELLANT IN NITROGEN
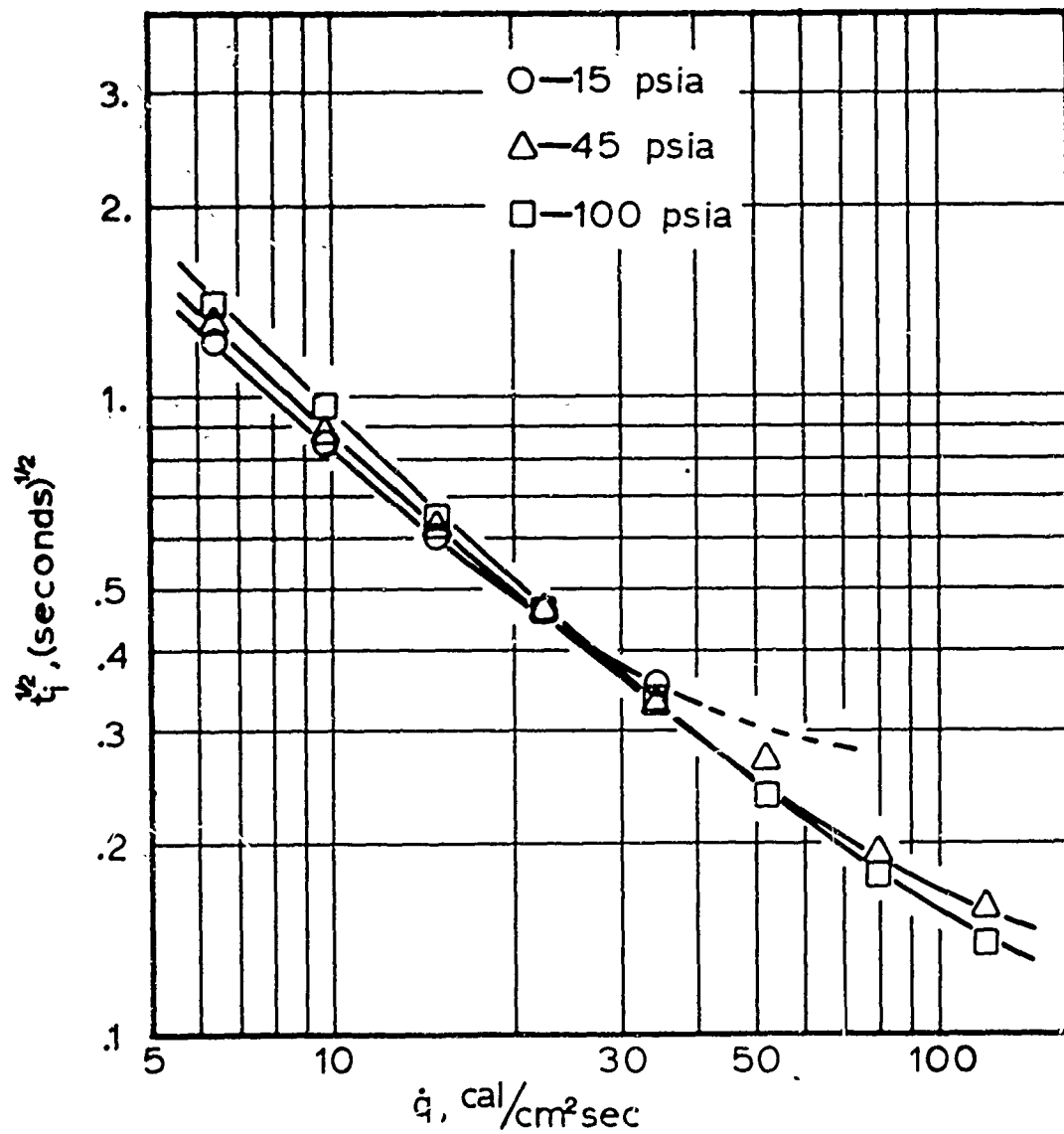AT TEST-GAS PRESSURES OF 15, 45 AND 100 PSIA.

FIGURE 10. IGNITION DATA FOR A-87 PROPELLANT IN METHANE
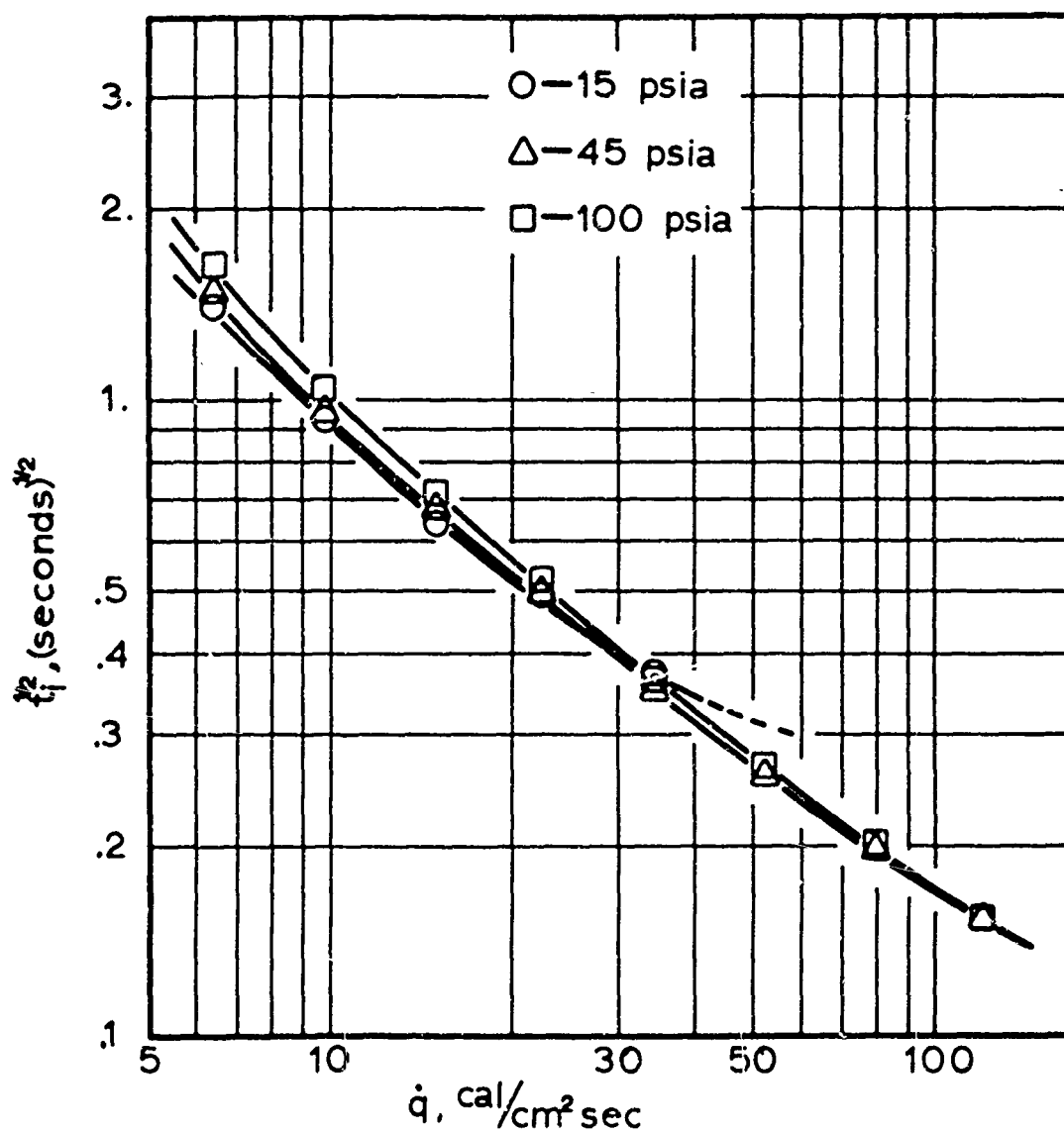AT TEST-GAS PRESSURES OF 15, 45 AND 100 PSIA.

30

FIGURE 11. IGNITION DATA FOR A-87 PROPELLANT
IN HELIUM AT TEST-GAS PRESSURES OF 15, 45 AND
100 PSIA.

oxygen also supports this view since, in the high oxidizer concentration of pure oxygen, diffusion requirements to satisfy the ignition reaction are easily met even at one atmosphere.

Compared to the other gases, the relative ease of ignition of A-87 in oxygen strongly suggests that, in addition to satisfying the diffusional requirements, the first propellant constituant to begin significant decomposition is the binder, with the first significant exothermic reaction occurring between the binder and environmental oxygen. Under the conditions of radiant heating, this is not surprising since the binder contains darkening agents (C and CC, which makes it a better absorber in this spectral range), and has a thermal diffusivity of about one-half that of AP.

In order to test the hypothesis of the first exothermic reaction occurring between binder pyrolysis products and oxidizer, a dummy propellant was formulated by substituting glass beads for the AP. Figure 12 shows the comparison of the ignition of the dummy propellant in oxygen, A-87 in oxygen and A-87 in nitrogen, with all tests run at 100 psia. The data scatter for the dummy propellant was much greater than for the propellant but within the scatter it is seen that the ignition time is nearly the same. In contrast, the ignition of A-87 in nitrogen (Fig. 9) is observed to take slightly longer at low flux, with the relative increase in ignition time becoming greater at high flux. This increased ignition time in nitrogen then is interpreted as being the additional time necessary for the AP to decompose sufficiently to meet the oxidizer concentration necessary for ignition.

It seems reasonable to suppose that the initial binder decomposition products may be light hydrocarbon fractions. To test this
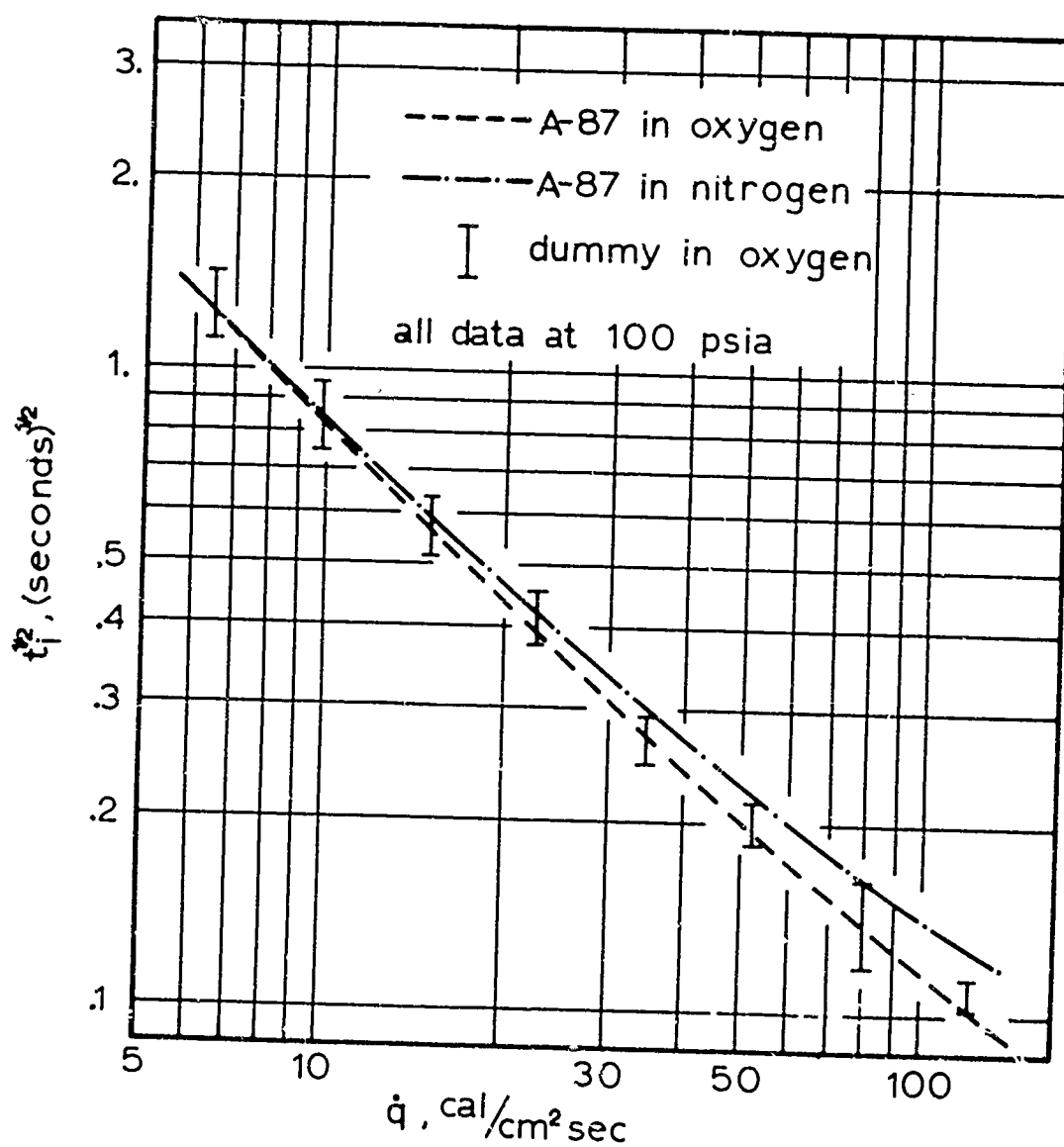
32

FIGURE 12. IGNITION DATA FOR THE DUMMY
INERT PROPELLANT IN OXYGEN. IGNITION
DATA FOR A-87 IN OXYGEN AND NITROGEN
SHOWN FOR COMPARISON.

33

hypothesis, pressed pellets of AP containing carbon and copper chromite but no binder were prepared, and ignited in methane. Results are shown in Fig. 13; and compared with the A-87 data in nitrogen. The data indicate that for radiant ignition in inert atmospheres the slow step in the process is the decomposition of AP to supply oxidizing gas species at a rate sufficient to allow ignition to occur. The trend is for the AP pellets to ignite easier at the higher heating rates in methane than the regular propellant sample (including binder) in nitrogen. This is reasonable from the diffusion argument since a diluent gas is not present to offer any barrier and the methane can easily meet the reaction diffusion requirements.

The preceeding discussion has evolved from an interpretation of the experimental results on terms of the influence of gaseous diffusion coupled with the relative rates of decomposition of propellant ingredients necessary to supply a reactable concentration of species in the gas phase. Other factors can also influence the observed trend of the experimental data.

For example, consider the problem of inferring the ignition time from the experimental data. The photodiode looks at the sample surface and the immediately adjacent gas phase region. The output signal strength of the detector, therefore, is a function of the rate of formation of self-luminous products formed in this region. This formation is expected to be exponentially dependent on temperature and at high heating rates (high flux) the contribution of the external heating in raising the temperature is greater than at lower heating rates (low flux). This is exaggerated at low pressure where low concentration of
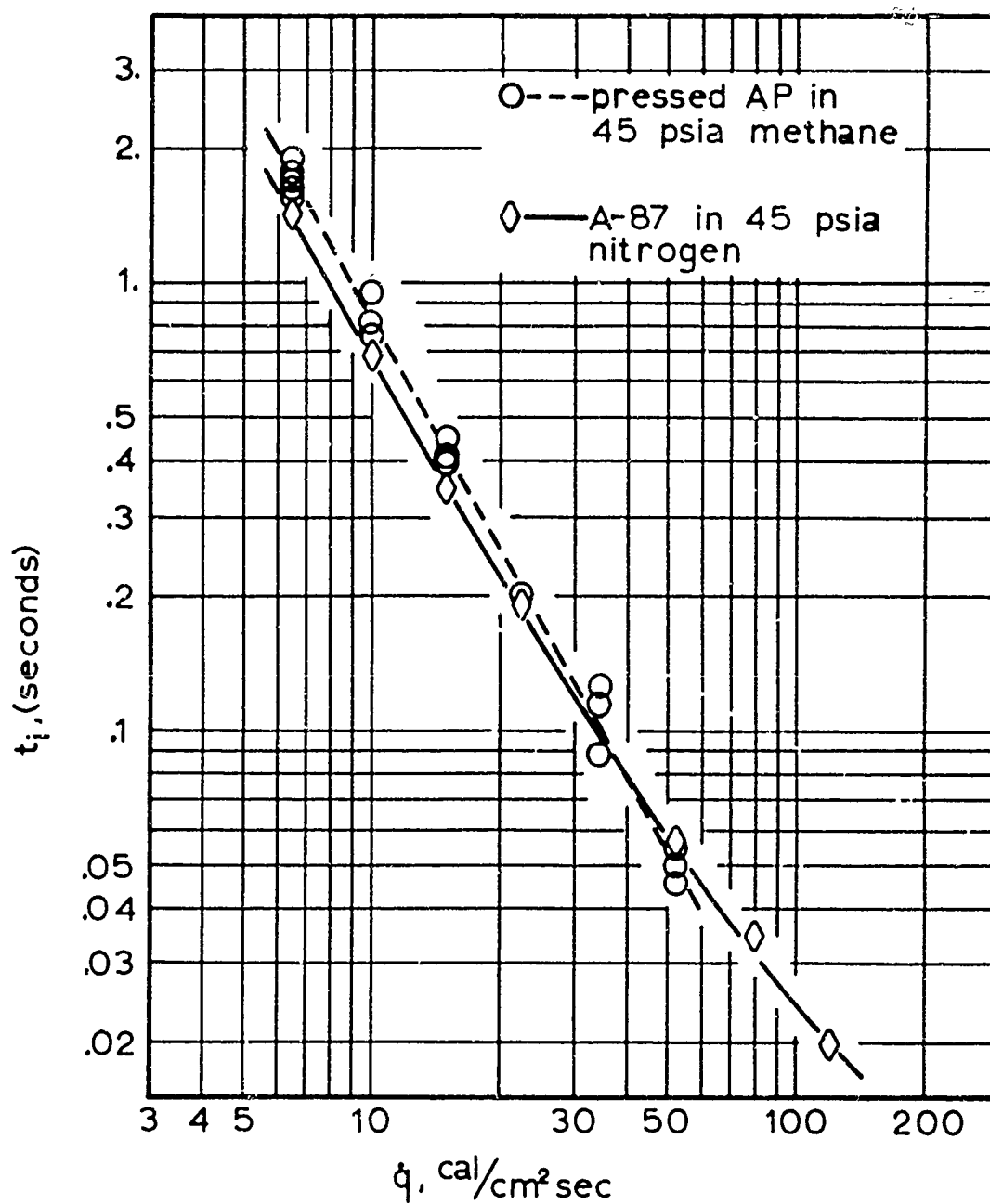
34

FIGURE 13. IGNITION DATA FOR PRESSED AP PELLETS
IN METHANE COMPARED TO THE IGNITION DATA FOR A-87
IN NITROGEN.

reactive species would delay the formation of self-luminous products.

The absorption of radiation in depth would also tend to make the slope of $\ln t^{\frac{1}{2}}$ vs. $\ln \dot{q}$ less than -1. The layer that would be conductively heated if all the energy was absorbed at the surface is thin under the condition of high flux and if appreciable absorption in depth occurred the thermal profile would be altered by an energy absorption-conduction coupled mechanism. This point is difficult to evaluate because a value of the optical extinction coefficient for composite propellants is not a simple exponential (due to optical heterogeneity). The binder of the propellant used in the present work is optically very dark, at least in the visible spectrum (the major portion of the radiant energy of the arc image furnace is in the visible spectrum), and it is expected that this effect would be small. If propellants are tested that are not optically dark this point would become increasingly important.

The present data indicate the trend of the pressure dependence is reversed at low fluxes compared to high fluxes; at high pressure the ignition time is longer than at low pressure at low fluxes. On a relative basis, this low flux pressure dependence is much less than the high flux pressure dependence, suggesting that a mechanism other than diffusion is becoming important.

Since there is a gas flow past the sample surface, it is likely that convective heat losses should become more important under the condition of low flux and longer ignition times. Heat transfer coefficients were estimated (see Appendix C) for the present test conditions and found to be consistant with this explanation of the low flux

36

dependence. For example, the ignition data of air at 6.45 cal/cm^2 sec

(see Table 3) indicates an increase in ignition time from 1.25 to 1.48

seconds at pressures of 15 and 100 psia respectively. From Table 2

the estimated heat transfer coefficients for the same respective con-

ditions are 2.3 x 10^{-4} and 3.7 x 15^{-4} cal/cm^2 sec. While it is proba-

ble that the heat loss due to convection is not the complete explan-

ation, it is believed to be a major factor contributing to the low

flux dependence.

SUMMARY OF RESULTS AND CONCLUSIONS

SUMMARY OF RESULTS

In summary, the data for ignition of a catalized, ammonium perchlorate composite propellant by high intensity thermal radiation shows that:

1. The effect of increasing the incident flux density is to decrease the ignition time with the maximum magnitude of the slope of $\ln t_i^{\frac{1}{2}}$ vs. $\ln \dot{q}$ always less than -1.

2. A dependence of ignition time on environmental gas pressure is found to be most pronounced at high flux densities with pure oxygen displaying the least pressure dependence of the environmental gases tested. A pure oxygen environment produced the shortest ignition time.

3. A different dependence of ignition time on oxygen concentration is observed if the concentration is changed by varying the mole fraction as compared to varying the total pressure.

4. The ignition time in inert atmospheres generally increases with decreasing molecular weight of the environment gas.

5. The ignition times of the dummy inert propellant in pure oxygen were the same as the ignition times for the live propellant in pure oxygen under the same test conditions.

6. The ignition time of pressed pellets of AP, copper chromite and carbon were approximately the same as the ignition time

of the live propellant in nitrogen under the same test
conditions.

CONCLUSIONS

From the results of this work, it is concluded that:

1. The simple model of an invariant surface temperature at
   ignition (i.e., neglecting any chemical self-heating) is
   inadequate to correlate experimental ignition data.

2. To explain the observed ignition data it is necessary
   to include the condition of chemical self-heating which
   can eventually become dominant over the externally supplied
   energy stimulus for ignition.

A qualitative extension of the condensed phase chemical heating
model of Price, et al [58] to the case of exothermic gas phase reac-
tions has shown that the expected trends of such a model are consistent
with the trends observed in the present experimental work. While the
qualitative arguments advanced are in agreement with the data of the
present work such agreement does not constitute proof of a particular
mechanism. The logic of the argument, however, strongly suggests that
under the experimental conditions of the present investigation exo-
thermic gas phase reactions play a role of major importance, if perhaps
not completely controlling, on the ignition of ammonium perchlorate
composite propellants with high intensity thermal radiation. Other
factors such as convective heat loss from the sample surface and radi-
ation absorption in depth can alter the dependence of ignition delay
on the external flux density.

39

RECOMMENDATIONS FOR FUTURE WORK

The following areas of investigation would supply additional information pertinent to the ignition processes of composite propellants:

1. The thermal decomposition of individual propellant ingredients should be investigated under the conditions of pressure and heating rates common to practical motor ignition conditions.

2. Different methods of detecting ignition should be thoroughly investigated. This would include such techniques as (a) the controlled exposure go-no go statistical method and (b) ionization probes.

3. The effect of different modes of external heating on the same propellant should be investigated over a wide range of pressure and external flux. Such studies with both radiant and convective heating and on both optically light and dark propellants are necessary in order to determine the effect of absorption of radiant energy with depth and heat losses from the surface. Possible changes in ignition mechanisms might also be detected.

4. The use of optical techniques such as motion picture photography and interferometric observation of the gas phase immediately above the propellant surface would be of great value in determining the mechanism of the ignition process.

5. Measurement of the propellant surface temperature during external heating could reveal important additional information about the ignition process.

BIBLIOGRAPHY

1. Allen, H., Jr., and M. L. Pinns. "Relative ignitability of typical solid propellants with chlorine trifluoride." <u>National Aeronautics and Space Administration</u>, NASA TN D-1533, 1963.

2. Altman, D. and A. F. Grant, Jr. "Thermal theory of solid-propellant ignition by hot wires." <u>Fourth Symposium (International) on Combustion</u>. Williams and Wilkins Co., Baltimore, Maryland, 1953. p. 158-161.

3. Altman, D. and P. L. Nichols, Jr. "Ignition of solid propellants" (U). Jet Propulsion Laboratory, <u>California Institute of Technology</u>, Pasadena, California, Report No. DA-04-495-ORD 18, September, 1954, CONFIDENTIAL.

4. Anderson, R., et al. "Critical comparison of solid propellant ignition theories." <u>United Technology Center</u>, Sunnyvale, California, TM-34-63-U2, August, 1963.

5. Anderson, R., R. S. Brown and L. J. Shannon. "Ignition theory of solid propellants." <u>American Institute of Aeronautics and Astronautics</u>, AIAA Preprint No. 64-156, January, 1964.

6. Anderson, R., R. S. Brown, G. T. Thompson and R. W. Ebling. "Theory of hypergolic ignition of solid propellants." <u>American Institute of Aeronautics and Astronautics</u>, AIAA Preprint No. 63-514, December, 1963.

7. Anderson, R., R. S. Brown, R. Ebling and R. W. Hawke. "Fundamental investigation of hypergolic ignition for solid propellants" (U). <u>United Technology Center</u>, Sunnyvale, California, UTC 2018-FR, CONFIDENTIAL.

8. Baer, A. D. <u>Ignition of composite rocket propellants</u>. Unpublished Ph.D. in Chemical Engineering, University of Utah, Salt Lake City, June, 1959.

9. Baer, A. D. and N. W. Ryan. "Ignition of composite propellants by low radiant fluxes." <u>American Institute of Aeronautics and Astronautics</u>, AIAA Preprint No. 64-119, January, 1964.

10. Baer, A. D., N. W. Ryan and D. L. Salt. "Propellant ignition by high convective heat fluxes." <u>Progress in Astronautics and Rocketry: Vol. 1. Solid Propellant Rocket Research</u>, edited by M. Summerfield, Academic Press, New York, 1960. p. 653-672.

11. Bastress, E. K., D. S. Allan and D. L. Richardson. "Solid propellant ignition studies." Arthur D. Little, Inc., Air Force Rocket Research Laboratories, Edwards Air Force Base, California, Technical Documentary Report No. RPL-TDR-64-65, Final Report, October, 1964, CONFIDENTIAL.

12. Beyer, R. B. and N. Fishman. "Solid propellant ignition studies with high flux radiant energy as a thermal source." Progress in Astronautics and Rocketry: Vol. I. Solid Propellant Research, edited by M. Summerfield, Academic Press, New York, 1960. p. 673-692.

13. Beyer, R. B., R. Anderson, R. O. MacLaren and J. J. Corcoron. "Ignition of solid-propellant motors under vacuum." United Technology Center, Sunnyvale, California, Final Report UTC-2079-FR, April, 1965.

14. Beyer, R., R. Anderson, and R. O. MacLaren. "UTC arc-imaging furnace." United Technology Center, Sunnyvale, California, TM-36-64-U1, October, 1964.

15. Beyer, R. B., L. McCulley and M. W. Evans. "Measurement of energy flux density distribution in the focus of an arc image furnace." Applied Optics, 5, 131-135 (1964).

16. Bircumshaw, L. L. and B. H. Newman. "The thermal decomposition of ammonium perchlorate: I. Introduction, experimental analysis of gaseous products and thermal decomposition experiments." Proceedings Roy. Soc. (London) Ser. A. 227, 115-132 (1954).

17. Bircumshaw, L. L. and B. H. Newman. "The thermal decomposition of ammonium perchlorate: II. The kinetics of decomposition, the effect of particle size, and discussion of results." Proceedings Roy. Soc. (London) Ser. A. 227, 228-241 (1954).

18. Bradley, H. H., Jr. and E. W. Price. "Tables of computer calculations for heating of an opaque, semi-infinite reactive solid by constant radiant flux, ignoring reactant consumption." U. S. Naval Ordnance Test Station, China Lake, California. Unpublished Technical Note TN 5008-17, December, 1963. (Computer solutions carried out by Stanford Research Institute)

19. ------. "Tables of computer calculations for heating of a reactive solid by constant radiant flux, including effect of depletion of reactant by chemical reaction of order 1/2, 1, and 3/2." U. S. Naval Ordnance Test Station, China Lake, California. Unpublished Technical Note TN 5008-18, July, 1964. (Computer solutions carried out by Stanford Research Institute)

20. ------. "Tables of computer calculations for heating of a reactive solid by constant radiant flux, including effects of depletion of reactants and of optical absorption of radiant energy in

depth." U. S. Naval Ordnance Test Station, China Lake, California. Unpublished Technical Note TN 5008-19, August, 1964. (Computer solutions carried out by Stanford Research Institute)

21. Broido, A. and A. B. Willoughby. "Measurement of intense beams of thermal radiation." Journal Op. Soc. Am., 48, 344-350 (May, 1958).

22. Churchill, S. W., R. W. Kruggel and J. C. Brier. "Ignition of solid propellants by forced convection." Am. Inst. Chem. Eng. Journal, 2, 568-571 (1956).

23. Evans, M. W., R. B. Beyer and L. McCulley. "Initiation of deflagration waves at the surfaces of ammonium perchlorate-copper chromite-carbon pellets." Journal Chem. Phys., 40, 2431-2438 (1964).

24. Frazer, J. H. and B. L. Hicks. "Thermal theory of ignition of solid propellants." Journal Phys. Colloid Chem., 54, 872-876 (1950).

25. Galway, A. K. and P. W. M. Jacobs. "The thermal decomposition of ammonium perchlorate at low temperatures." Proceedings Roy. Soc. (London) Ser. A 254, 455-469 (1960).

26. Galway, A. K. and P. W. M. Jacobs. "The thermal decomposition of ammonium perchlorate in the presence of carbon." Transactions Faraday Soc., 56, 581-590 (1960).

27. Gardon, R. "An instrument for the direct measurement of intense thermal radiation." Review Sci. Instruments, 24, 366-370 (1953).

28. Glaser, P. E. "High radiation-flux, absolute, water-flow calorimeter." Review Sci. Instruments, 28, 1084-1086 (1957).

29. Glaser, P. E. "Imaging-Furnace developments for high-temperature research." Journal Electrochem. Soc., 107, 226-231 (1960).

30. Grant, E. H., Jr., R. W. Lancaster, J. Wenograd and M. Summerfield. "A study of the ignition of solid propellants in a small rocket motor." American Institute of Aeronautics and Astronautics, AIAA Preprint No. 64-153, January, 1964.

31. Grant, E. H., Jr., J. Wenograd and M. Summerfield. "Research on solid propellant ignitability and igniter characteristics." Princeton University, Department of Aeronautical Engineering, Aeronautical Engineering Report No. 662, October, 1963.

32. Hermance, C. E., R. Shinnar, J. Wenograd and M. Summerfield. "Solid propellant ignition studies: ignition of the reaction field adjacent to the surface of a solid propellant."

44

Princeton University, Department of Aerospace and Mechanical Sciences, Aeronautical Engineering Report No. 674, December, 1963.

33. Hermance, C. E., R. Shinnar and M. Summerfield. "Ignition of an evaporating fuel in a hot, stagnant gas containing an oxidizer." AIAA Journal, 3, 1584-1592 (September, 1965).

34. Hicks, B. L. "Theory of ignition considered as a thermal reaction." Journal Chem. Phys., 22, 414-429 (1954).

35. Hiester, N. K. and R. E. Dela Rue. "The image furnace as a research tool." ARS Journal, 30, 928-938 (October, 1960).

36. Jacobs, P. W. M. and A. R. T. Kureishy. "The effect of additives on the thermal decomposition of ammonium perchlorate." Eighth Symposium (International) on Combustion. Williams and Wilkins Co., Baltimore, Maryland, 1962. p. 672-677.

37. Jacobs, P. W. M. and A. R. T. Kureishy. "Thermal ignition in the system ammonium perchlorate-cuprous oxide." Journal Chem. Soc., 555-561 (1962).

38. Jenkins, R. J. and C. P. Butler. "The stability and reproducibility of a carbon arc image furnace." Applied Optics, 4, 299-302 (March, 1965).

39. Keller, J. A. Studies on ignition of ammonium perchlorate-based propellants by convective heating. Ph.D. in Chemical Engineering, University of Utah, Salt Lake City, August, 1965.

40. Keller, J. A., A. D. Baer and N. W. Ryan. "The ignition of composite propellants by hot gases." Western States Section of the Combustion Institute. WSS/CI Paper 64-27, October, 1964.

41. Keller, J. A., C. P. Richardson, A. D. Baer and N. W. Ryan. "Final technical report on propellant ignition by convective heat fluxes." University of Utah, Department of Chemical Engineering, Salt Lake City, Utah, 28 June 1963 to 30 September 1964.

42. Kling, R., A. Maman and J. Brulard. "The kinetics of the ignition of composite solid propellants submitted to high heat fluxes." Rech. Aerosp., 103, 3-10 (1964).

43. Kreith, Frank. Principles of heat transfer. 4th printing. Scranton, Pennsylvania, International, 1961. p. 268.

44. Kutatani, K. "Some studies on solid propellant; Part I. Kinetics of the thermal decomposition of ammonium perchlorate." Aeronautical Research Institute, University of Tokyo (In English), July, 1962.

45. Lancaster, R. W. and M. Summerfield. "Experimental investigation of the ignition process of solid propellants in a practical motor configuration." _Princeton University_, Department of Aeronautical Engineering, Aeronautical Engineering Report No. 548, AFOSR TN 836, May, 1961.

46. Laszlo, T. S. _Image furnace techniques._ Technique of Inorganic Chemistry, Vol. V. Interscience Publishers, div. of Wiley, New York, 1965.

47. Lovine, R. L., L. Y. Fong and B. E. Paul. "Diffusional analysis of composite propellant ignition and its application to solid rocket ignition." _American Institute of Aeronautics and Astronautics_, AIAA Preprint 64-117, January, 1964.

48. McAlevy, R. F., III. _The ignition mechanism of composite solid propellants._ Unpublished Ph.D. in Aeronautical Engineering, Princeton University, Princeton, 1960.

49. McAlevy, R. F., III, P. L. Cowan and M. Summerfield. "The mechanism of ignition of composite solid propellants by hot gases." _Progress in Astronautics and Rocketry: Vol. 1, Solid Propellant Rocket Research_, edited by M. Summerfield, Academic Press, New York, 1960. p. 623-652.

50. McAlevy, R. F., III, and M. Summerfield. "Ignition of double-base solid rocket propellants." _Am. Rocket Soc. Journal_, 32, 270-273 (1962).

51. McAlevy, R. F., III, and J. G. Hansel. "Linear pyrolysis of thermoplastics in chemically reactive environments." _AIAA Journal_, 3, 243-249 (1965).

52. McAlevy, R. F., III, S. Y. Lee and R. S. Magee. "The solid propellant ignition mechanism: A simple diagnostic experiment." _Astronautica Acta_, 11, 144-145 (1965).

53. McCune, C. C. _Solid propellant ignition studies in a shock tube._ Unpublished Ph.D. in Chemical Engineering, University of Utah, Salt Lake City, August, 1961.

54. Mitchell, R. C., J. A. Keller, A. D. Baer and N. W. Ryan. "Ignition of solid propellants." _University of Utah_, Department of Chemical Engineering, AFOSR 62-99, 1962.

55. Niessen, W. R. and E. K. Bastress. "Solid propellant ignition studies." _Arthur D. Little, Inc._, Cambridge, Massachusetts, _First Quarterly Technical Documentary Report_ No. AFRPL-TR-65-136, July, 1965.

56. Null, M. R. and W. W. Lozier. "Carbon arc image furnaces." _Review of Sci. Inst._, 29, 163-170 (February, 1958).

46

57. Olds, R. H. and G. B. Shook. "Mathematical study of thermal processes relating to reaction rates in solid fuels." U. S. Naval Ordnance Test Station, China Lake, California, Technical Memorandum 917, June, 1952.

58. Price, E. W., H. H. Bradley, Jr., and R. Fleming. "Ignition of solid propellants." Western States Section of the Combustion Institute. WSS/CI Paper 63-6, April, 1963.

59. Price, E. W., H. H. Bradley, Jr., G. L. Dehority and M. M. Ibiricu. "Theory of ignition of solid propellants." AIAA Journal, 4, 1153-81 (July, 1966).

60. Price, E. W., H. H. Bradley, Jr., J. D. Hightower and R. O. Fleming, Jr. "Ignition of solid propellants." American Institute of Aeronautics and Astronautics, AIAA Preprint No. 64-120, January, 1964.

61. Roth, J. F. and G. P. Wachtell. "Heat transfer kinetics in the ignition of solid propellants." Ind. Eng. Chem., Fundamentals 1, 62-67 (1962).

62. Ryan, N. W., A. D. Baer, J. A. Keller and R. C. Mitchell. "Ignition and combustion of solid propellants." University of Utah, Department of Chemical Engineering, Final Technical Report, AFOSR 2225, September, 1961.

63. Ryan, N. W., A. D. Baer, J. A. Keller and R. C. Mitchell. "Ignition and combustion of solid propellants." University of Utah, Department of Chemical Engineering, Technical Report AFOSR 62-69, September, 1962.

64. Ryan, N. W., A. D. Baer and J. A. Keller. "Ignition and combustion of solid propellants." University of Utah, Department of Chemical Engineering, Technical Report AFOSR 40-64, September, 1964.

65. Schneider, P. J. Temperature response charts. New York, Wiley, 1963. p. 119.

66. Summerfield, M. and R. F. McAlevy, III. "The shock tube as a tool for solid propellant ignition research." Jet Propulsion, 28, 478-481 (1958).

67. Summerfield, M., R. Shinnar, C. E. Hermance and J. Wenograd. "A critical review of recent research on the mechanism of ignition of solid propellants." Princeton University, Department of Aeronautical Engineering, Aeronautical Engineering Laboratory Report No. 661, AF-AFOSR-92-63, August, 1963.

68. Thomas, P. H. "Some conduction problems in heating small areas on large solids." Quart. Journal Mech. and Appl. Math, 10, 482-93 (1957.

69. Von Elbe, Guenther. "Theory of solid propellant ignition and response to pressure transients." In Bulletin of the Inter-agency Solid Propellant Group Meeting, Alexandria, Virginia, Atlantic Research Corporation, Vol. III, 95-127, July, 1963.

70. Williams, F. A. and H. Barrere. "Ignition of Solid Propellants." In Second Interagency Chemical Rocket Propulsion Group Combustion Conference, comp. and ed. by Chemical Propulsion Information Agency, Silver Spring, Md., CPIA Publ. No. 105, Vol. 1, May, 1966.

71. Willoughby, A. B. "Absolute water flow calorimeter for the measurement of intense beams of radiant energy." Review Sci. Inst., 25, 667-670 (July, 1954).

72. Yang, C. H. "Theory of ignition and auto-ignition." Combustion and Flame, VI, 215-225 (July, 1962).

APPENDIX A

EXPERIMENTAL DETAILS

FURNACE SOURCE AND OPTICAL DETAILS

An overall view of the furnace is shown in Fig. 14, while Fig. 15 shows the details of the interior of the lamp house with the xenon bulb, primary mirror, auxiliary mirror and the mirror adjustment controls. The radiation source is an Osram 2,500 watt xenon bulb mounted in a Strong X-1600 movie projection lamp house (type 76002-2) and radiating at a color temperature of approximately 6,000°K. The primary mirror is a glass, 14-inch diameter, first surface, aluminized ellipsoidal mirror which produces an image of the arc source at the second focal point with a magnification of approximately 5X. After being collected by the second mirror the beam converges to a focal volume roughly the size of the arc source. The auxiliary mirror is used to increase the energy-gathering efficiency of the system by collecting the energy radiated from the front of the xenon arc and refocusing it back through the arc plasma to the primary mirror. The spectral distribution of energy radiated from the arc is shown in Fig. 16. It can be seen that most of the energy lies between 0.3 and 1.1 microns with several peaks in the near infrared between 0.8 and 1.0 microns. Bastress [11] has studied the effect of spectral distribution on propellant ignition and found no noticeable effect, which suggests that photochemical processes are not important in composite propellant ignition.

FIGURE 14. OVERALL VIEW OF ARC IMAGE FURNACE FACILITY.
THE SECONDARY MIRROR AND IGNITION BOMB CAN BE SEEN AT
RIGHT. THE LAMPHOUSE IS SHOWN AT LEFT WITH THE SHUTTER
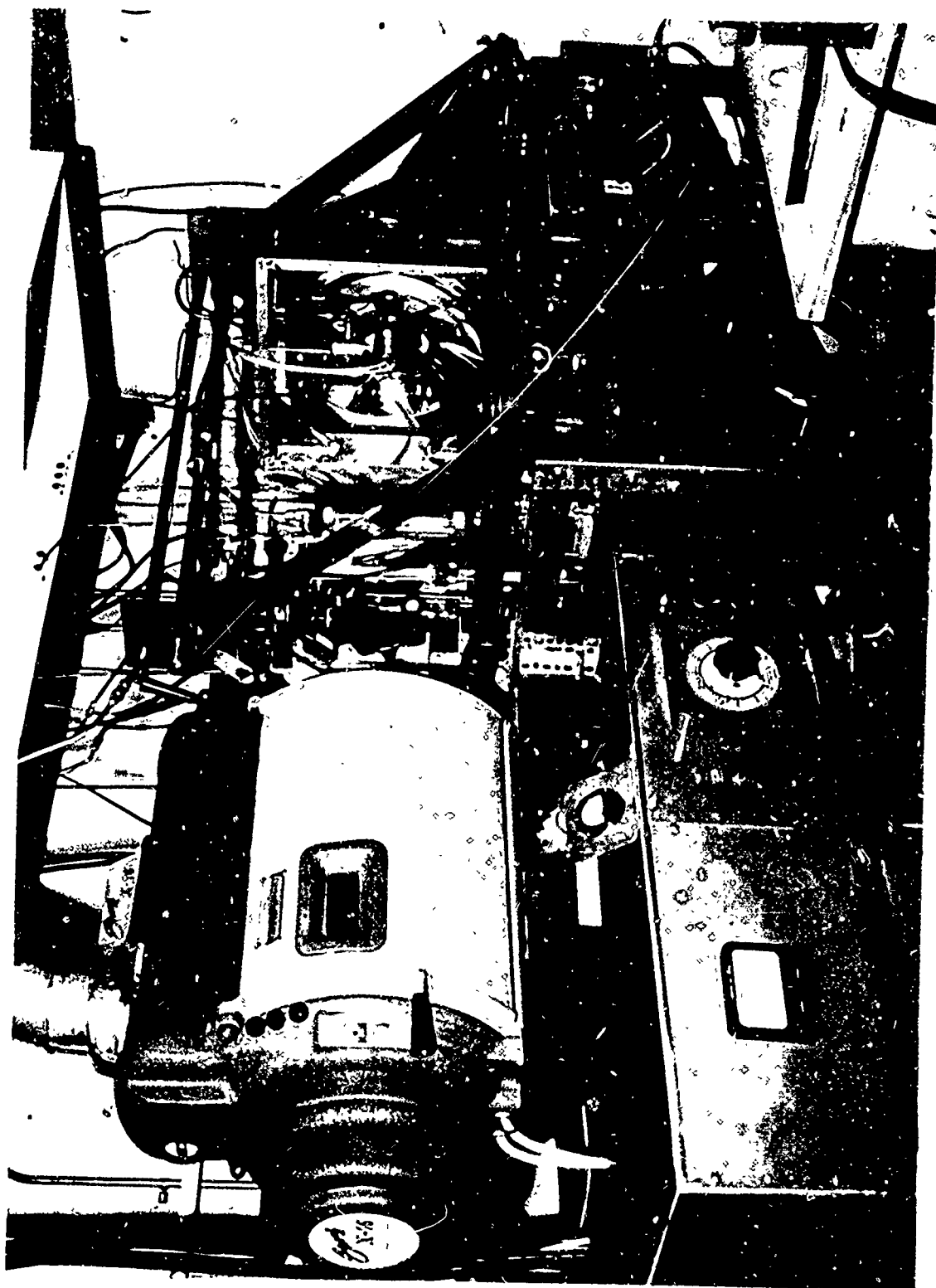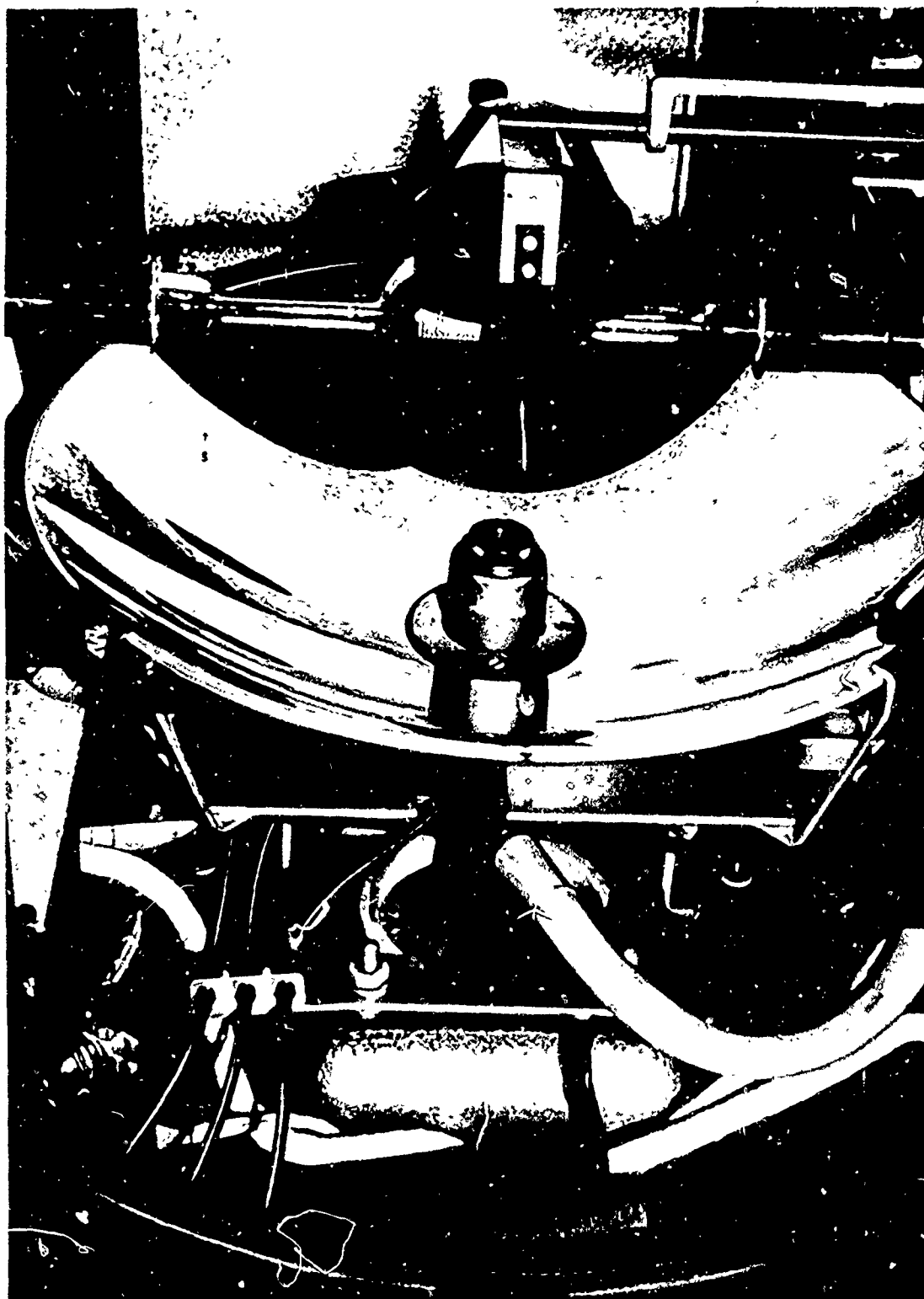MECHANISM IN THE CENTER.

FIGURE 15. INTERIOR VIEW OF LAMPHOUSE SHOWING THE XENON LAMP, PRIMARY AND AUXILIARY MIRRORS, AND MIRROR POSITION CONTROLS.
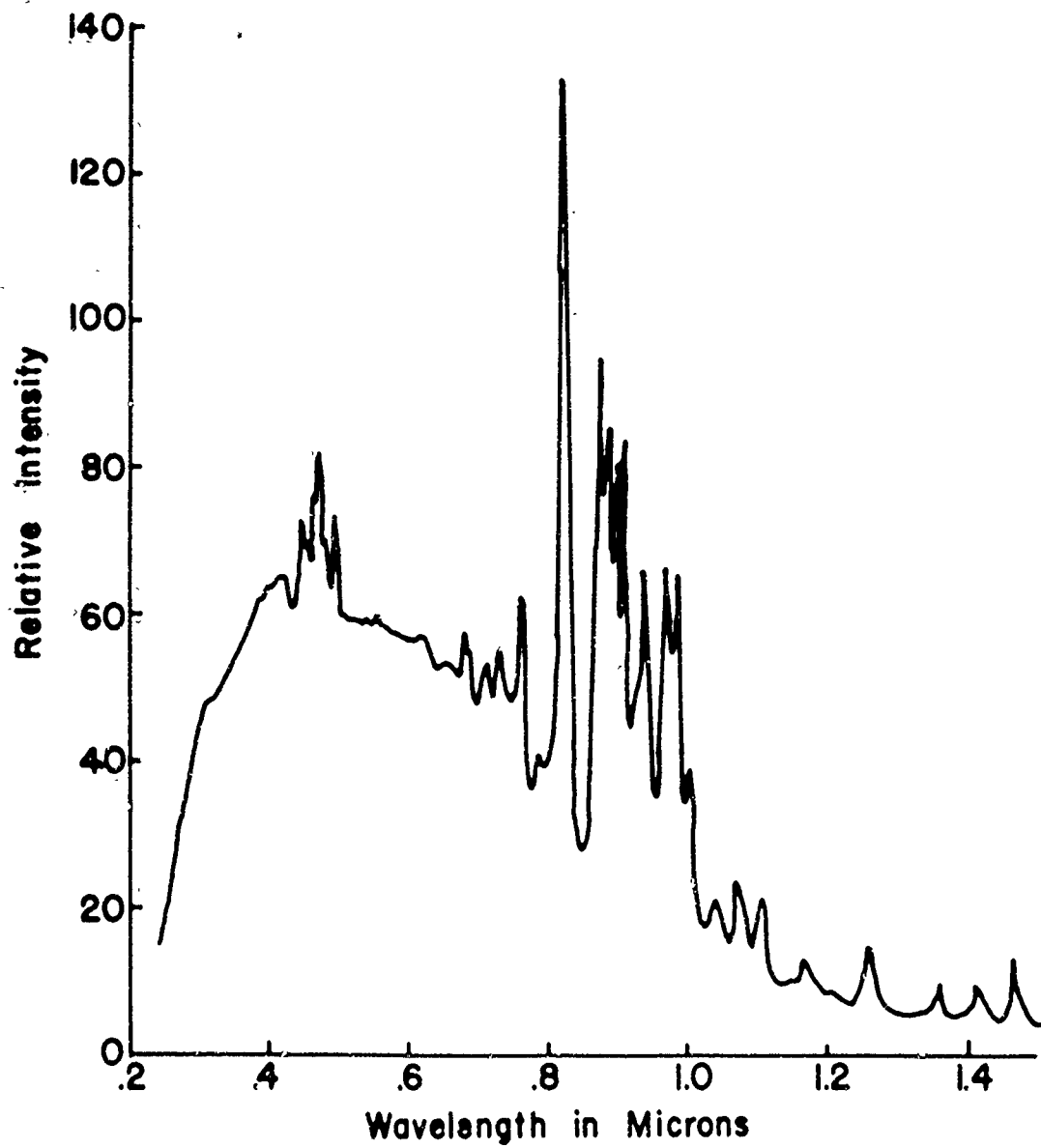
FIGURE 16. SPECTRAL DISTRIBUTION OF RADIANT
ENERGY FROM OSRAM 2,500 WATT XENON LAMP.

The arc power supply is of the selenium rectified d-c type utilizing three-phase, full-wave bridge rectifiers. The output current is controlled remotely at the furnace. Lamp current ripple is limited to approximately 3 percent. The output is not regulated and laboratory line voltage fluctuations are readily noted on the arc current meter. Figure 17 shows the variation of measured flux density as a function of lamp current. The lamp current meter is carefully monitored visually during each ignition run and if the current is observed to fluctuate by more than ± 1 amp the run is rejected. Within the limitations imposed by reading the meter, flux variations during any one run are thus limited to approximately ± 2 cal/cm^2 sec.

Although the source has proven to be extremely stable and reproducible, there are two other factors that can influence reproducibility. First, the elliptical mirror system has an effective speed of approximately f/.3 and small variations in the relative location of sample to second mirror can cause significant variation of the flux intensity at the sample. Second, it has been noted that following initial arc strike a definite warm-up time is required for the lamp to reach steady state operation and for the primary and auxiliary mirrors to reach thermal equilibrium (which produces an optical distortion compared to "cold" mirrors). Figure 18 shows the variation in measured flux density as a function of time following initial striking of the arc. The first of these problems is minimized by using a very rigid test chamber, mechanical positioner and second mirror mount. The problem of flux variation due to thermal expansion and warm-up is circumvented by allowing sufficient time (at least 5 minutes) to elapse after striking
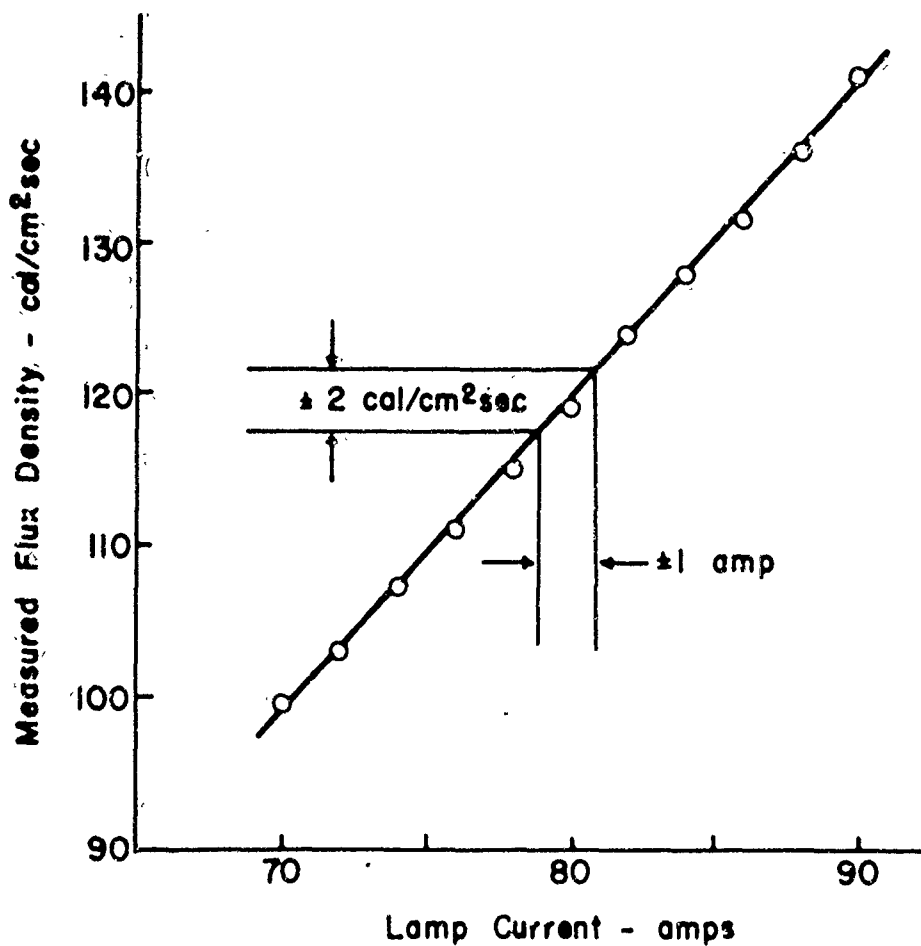
55

FIGURE 17. VARIATION OF THE MEASURED FLUX DENSITY VS.
LAMP CURRENT. MEASUREMENTS WERE MADE INSIDE THE IGNI-
TION BOMB AT A SPATIAL LOCATION CORRESPONDING TO THE
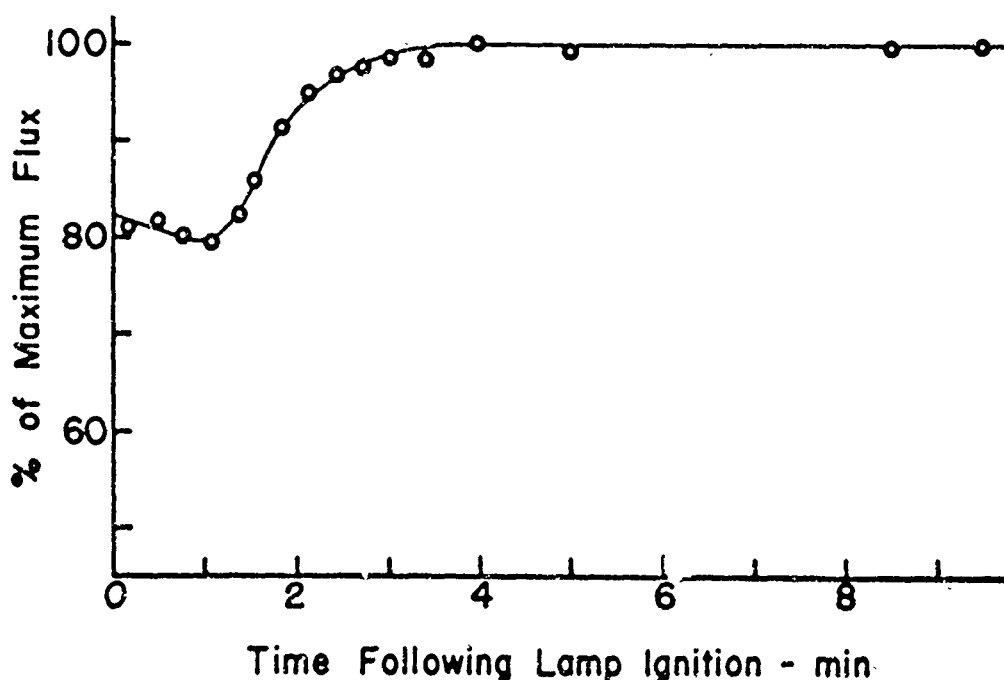CENTER OF THE EXPOSED PROPELLANT SAMPLE.

FIGURE. 18. INITIAL WARM-UP CHARACTERISTICS OF THE OSRAM 2500 WATT XENON LAMP AND ASSOCIATED OPTICAL COMPONENTS.

the arc. Normally, to conserve time once the arc is struck, the lamp is run continuously for the entire test period (up to 4 hours).
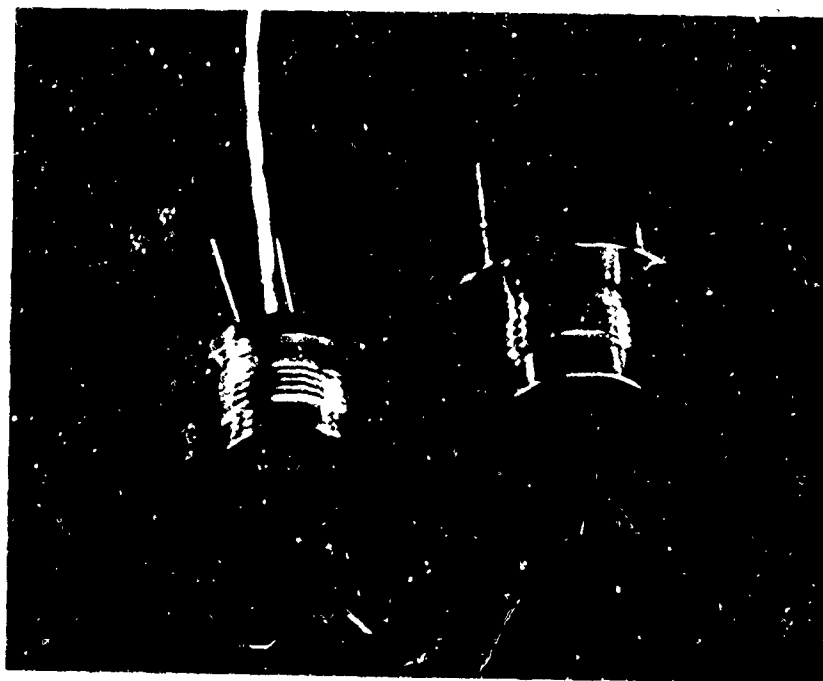
IGNITION CHAMBER AND SAMPLE HOLDER

The ignition chamber used in these studies is shown in Fig. 19a. This chamber consists of a stainless steel housing with a 1/2-inch thick fused quartz window to allow transmission of the radiant energy to the propellant sample. A 0.042-inch thick by 2 13/32-inch square disposable silica glass sheet is placed next to the quartz window between the window and the sample to protect the quartz from hot propellant gases following ignition. The propellant sample is mounted 1/2 inch behind the quartz-glass combination window and flush with the back wall of a rectangular cross-section environmental gas flow channel.

FIGURE 19. a. MAIN BODY OF IGNITION BOMB SHOWING THE
SAMPLE HOLDER IN PLACE WITH A PROPELLANT SAMPLE IN THE
CENTER. ENVIRONMENTAL GASES ENTER AT THE BOTTOM AND
FLOW UPWARDS THROUGH THE RECTANGULAR CHANNEL. BOMB
PRESSURE TAP AT LEFT AND PHOTODIODE COAXIAL CONNECTOR
AT RIGHT. b. RADIOMETER FOR FLUX MEASUREMENTS (LEFT)
AND SAMPLE HOLDER (RIGHT) ARE INTERCHANGEABLE IN THE
BOMB.
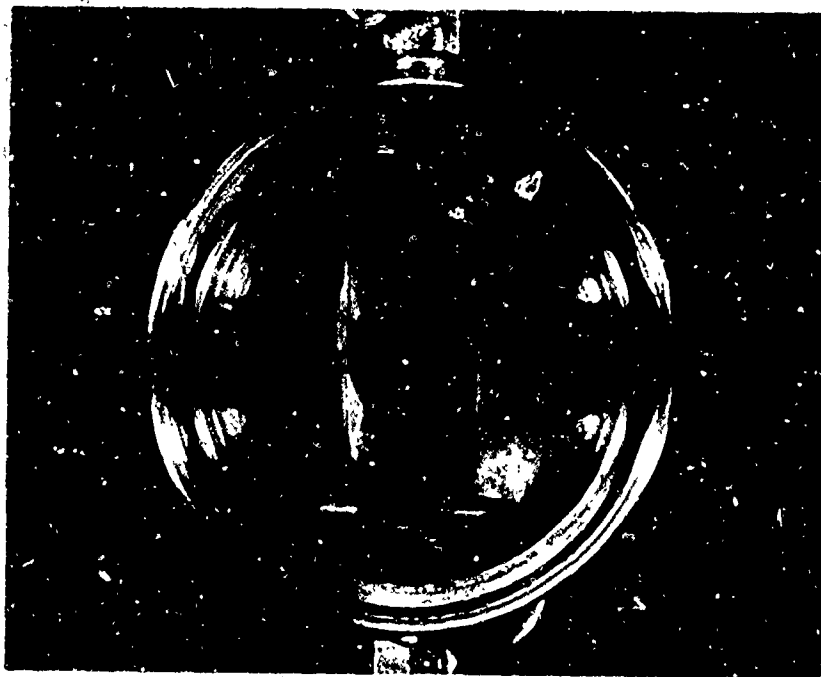
a. Main Body of Ignition Bomb.

b. Radiometer (Left) and Sample Holder (Right).

The environmental gas is admitted at the bottom of the chamber and after passing through a set of porous stainless steel plates flows vertically upwards past the sample surface. A photodiode is aligned parallel with and looks across the propellant surface to detect the appearance of a luminous exothermic reaction. The ignition chamber is mounted on a three axis mechanical positioner such that the flux distribution can be mapped and the specimen location can be made coincident with the maximum flux density location.

The sample holder is cylindrical in shape and fits into the back of the ignition chamber such that the flat circular end that holds the propellant sample is flush with and forms part of the environmental gas flow channel. A cylindrical hole 0.25 inches in diameter and 0.125 inches deep, located in the center of the circular end of the sample holder, is used to hold the propellant sample. Flux density measurements are made with a radiometer with the same external dimensions as the sample holder and with the thermal sensing area occupying the same relative position as the center of the propellant sample. Figure 19b shows the general configuration of the sample holder and radiometer.

SAMPLE PREPARATION

The preparation of the sample surface is very important from the standpoint of reproducibility. Imperfections on the propellant surface resulting from the preparation procedure can lead to non-typical ignition behavior by providing sites for three-dimensional heat transfer. Sample surfaces prepared by machining, cutting with a microtome and cutting with a razor blade were inspected under a stereomicroscope. The machined surface appeared to be the least desirable with more

60

evidence of crushed crystals and general surface roughness than either of the cut surfaces. Neither of the cut surfaces seemed to be better than the other in general appearance. In either case, it was impossible to obtain a microscopically smooth surface. Surface roughness is estimated to be on the order of 5 or 10 microns.

Since the razor cut technique is by far more convenient, it has been used throughout the testing. Preparation of the specimen is accomplished by firmly pushing a slightly oversize propellant slug into the specimen holder and slicing the excess propellant off with a clean, sharp razor blade. For this operation the razor blade is guided by the flat front surface of the specimen holder. By firmly pushing the sample into the sample holder and slicing off the excess propellant, the exposed sample surface is flat and lies in the same plane as the surface of the sample holder. This type of sample preparation insures that the propellant sample will not receive radiation on a corner edge. If a sample is heated on a corner non-one-dimensional heating will occur which under some conditions could produce unrealistic ignition results. Baer and Ryan [9, 61] have shown that heating of a 90° corner will be twice as fast for a given flux as heating of a one-dimensional propellant surface. Each prepared specimen is examined under a stereo-microscope to insure that gross rough spots or propellant edges are not present that would tend to cause misleading ignition behavior. Each sample is prepared in this manner, just prior to making a test, to insure a fresh propellant surface, thereby eliminating surface aging effects.

RADIATION FLUX DENSITY MEASUREMENT

The measurement of thermal radiation flux density in the range used in this work (6.5 to 120 cal/cm sec) presents a problem since standards for comparison and calibration are not available. This necessitates the use of a measuring instrument with an output signal that is proportional to the flux density incident on its sensing surface. In this general range of flux densities, two types of instruments have been used successfully: (1) absolute calorimeters which allow calculation of the flux density from directly measurable physical quantitites, or (2) radiometers which must be calibrated against an absolute calorimeter. Each of these instruments have advantages and disadvantages and the use of a particular type is dictated by the application. The characteristics of arc image furnaces which influence the choice of a particular type of instrument will be discussed briefly in the following section. A fairly complete description of high intensity flux density measuring instruments is given in Reference [46].

The radiant flux density varies in space within the focal volume in a manner prescribed by the spatial variation of the radiance of the arc source and the distortion caused by the optics of the system. The flux distribution at the focal volume of the arc image furnace is quite steep with the dimensions of the cross-section that defines at least 90 percent of peak flux density - being on the order of 0.050 inches. Thus, one requirement of an instrument to measure flux density is that it must have a sensing area sufficiently small to adequately resolve the space-density variation. To the extent that the arc source is unsteady, the flux density may vary with time. Therefore, it is highly

62

desirable to have a flux measuring instrument that has a relatively
fast response time so that some measure of the time variation can be
made.

Generally speaking, calorimeters do not fulfill the two require-
ments of space resolution and rapid response although the shielded slug
calorimeter [15] can be employed over a limited range of flux density
with a high degree of precision. A radiometer suitable for measuring
the flux density distribution near the focal point of an arc image
furnace with both adequate space and time resolution has been devised
by Gardon [27] and is available commercially from Hy-Cal Engineering,
Santa Fe Springs, California. Basically, the radiometer consists of a
thin metal foil disk supported around its periphery by a large, high
thermal diffusivity metal heat sink (usually water cooled). Attached
to the center of the back side of the thin foil disk is a fine wire
which forms a thermocouple junction at the point of attachment to the
foil. The radiometer is thus a differential thermocouple circuit which
measures the temperature gradient between the center and edge of the
foil. For a uniform flux density the temperature gradient from the
center to the edge of the foil, and hence the differential thermocouple
output signal, is directly proportional to the flux density.

Flux measurements in the present work were made with a Hy-Cal
radiometer model C-1301-A-300. This instrument was supplied with a
continuous point calibration in the range of 0 to 300 BTU/ft^2 sec
(80 cal/cm^2 sec). The accuracy is guaranteed to ± 2 percent and the
repeatability to $\pm$ 0.5 percent. The calibration supplied with the
instrument was linear and the slope of the calibration curve was used

63

to obtain a sensitivity of the instrument. The original calibration of the instrument was in terms of absorbed flux density. In order to obtain incident flux density values it is necessary to know the value of the absorbtivity of the receiver surface coating. A value of 0.89 was supplied by the manufacturer for their "special" high emissivity graphite coating. This coating was observed to deteriorate after several exposures to flux densities in the neighborhood of 100 cal/cm^2 sec and it was felt that it would be necessary to find a commercially available coating material which could be easily replaced at the first sign of deterioration. A product with the trade name "black velvet" manufactured by the Minnesota Mining and Manufacturing Company has been found to be entirely satisfactory. An experimental comparison "black velvet" with the original graphite coating indicated an absorption of 0.95 for the 3M material. This coating has been used throughout the present work.

Using the value of 0.95 for the absorbtivity of the surface coating the radiometer sensitivity for incident flux density was calculated to be 8.39 cal/cm^2 sec per mv. Even though the instrument was only calibrated to a value of about 80 cal/cm^2 sec it was assumed that the calculated sensitivity would be valid up to the maximum flux density of 120 cal/cm^2 sec used in this work. Since the temperature distribution of the thin foil is primarily due to conductive coupling to the heat sink, this would seem to be a valid assumption. Figure 22 shows that an extrapolation of the flux values in the range covered by the calibration supplied with the instrument are valid at least to 1.0 cal/cm^2 sec. A comparison of the radiometer with a shielded slug

64

calorimeter similar to the one described by Beyer, Evans and McCulley
[15] also showed the radiometer output-incident flux density relation-
ship to be the same as Fig. 22.

The sensing area of this model radiometer is 0.9 mm diameter
with a response time on the order of 100 milliseconds. The output
voltage at maximum flux density was 14.3 millivolts. This signal was
recorded on a Mosley Autograph X-Y recorder, Model 2DR, with an input
resistance of 2×10^5 ohms per volt. The accuracy of the recorder is
reported to be better than 0.20 percent of full scale with repeata-
bility better than 0.1 percent of full scale.

FLUX DENSITY DISTRIBUTION

The spatial distribution of the flux density was mapped inside
the ignition bomb with the water-cooled radiometer described above.
The radiometer, shown in Fig. 19b with the sample holder, is mounted in
a fixture of identical geometry as the sample holder such that the
sensing area of the radiometer will occupy the same spatial position
in the bomb as does the center of the propellant sample. Figure 20
shows the flux density profile that was measured with the bomb fully
assembled. The sample surface then receives a flux density constant
to ± 5 percent over an elliptical shaped area roughly 1.0 mm by 1.8 mm.

FLUX ATTENUATION

The arc source is operated at a constant current level and
energy output with the flux level at the sample being varied by mechan-
ical attenuation of the energy beam. The attenuation is accomplished
by placing various combinations of metal mesh screens at a predetermined
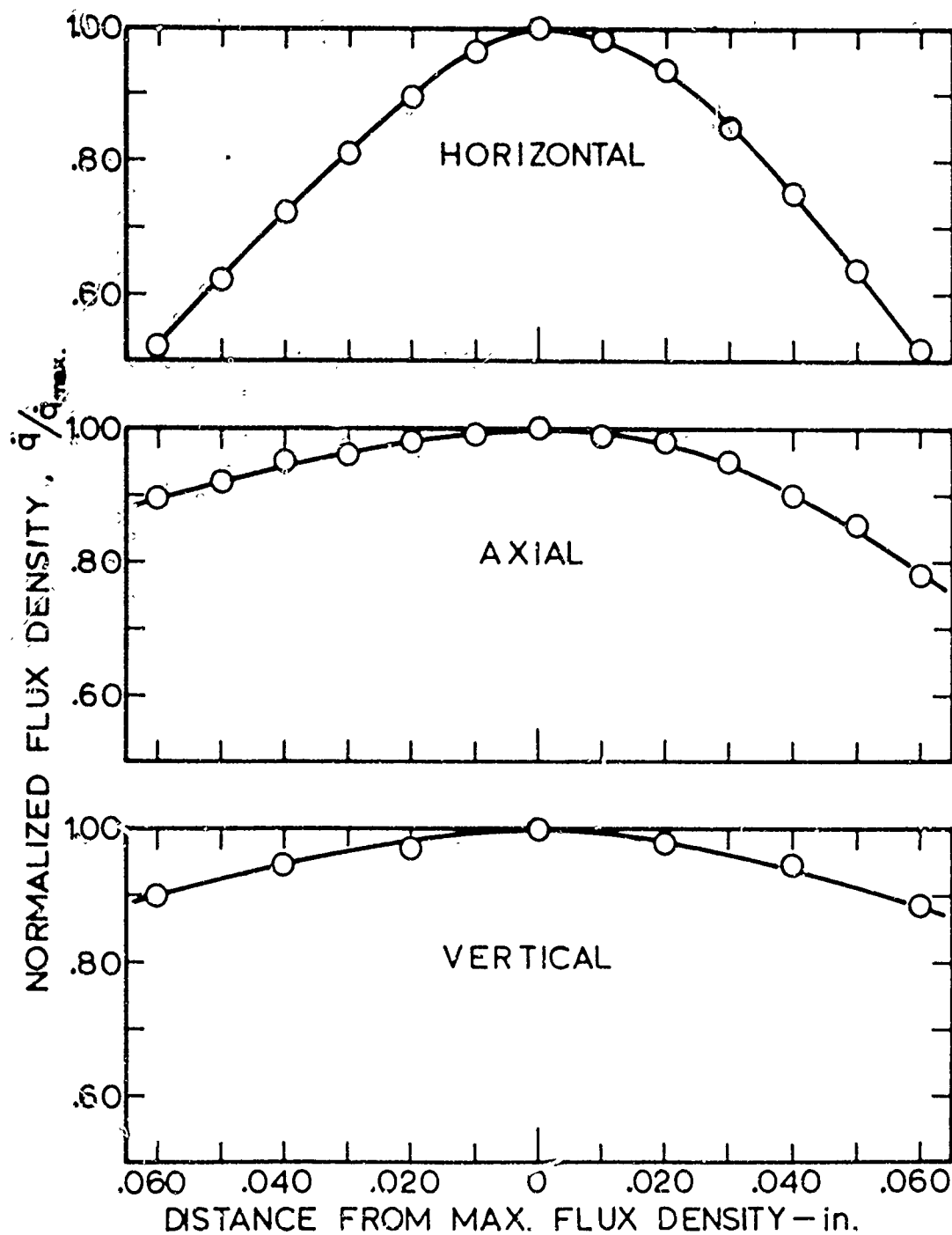
FIGURE 20.   FLUX DENSITY DISTRIBUTION AT THE FOCAL POINT
OF THE SECONDARY MIRROR.   OSRAM 2,500 WATT XENON LAMP
OPERATING AT A CONSTANT CURRENT OF 80 AMPS USED AS THE
SOURCE.

66

location in the diverging portion of the beam. The various mesh com-
binations are calibrated at a position well away from any of the opti-
cal focal points (approximately midway between the shutter position and
the secondary mirror) to avoid imaging of the mesh pattern on the
sample. A special attenuating screen location fixture is permanently
fixed to the furnace table to insure proper relocation of the screens
at their respective calibration positions. Figure 21 shows one of the
screens in position. A small blower is used to direct a gentle air
flow through the screens during exposure (see Fig. 27). Figure 22
shows the flux attenuation for different screen combinations used in
this work.

IGNITION DETECTION

The detection of self-luminosity from exothermic reactions at or
near the propellant sample surface is accomplished with a germanium
photodiode, type PHG-2, supplied by Nucleonic Products Company, Inc.,
Los Angeles, California. The relative spectral response of this photo-
diode is shown in Fig. 23. The optical axis of the photodiode is
aligned parallel with and approximately 1/16 inch above the sample sur-
face and look across the center of the sample. A sketch of the cross
section of the flow channel, propellant sample and photodiode is shown
in Fig. 24. The photodiode "sees" the propellant surface at a low
grazing angle and approximately 0.15" gas phase immediately above the
sample surface.

The output signal of the photodiode is fed into a Ken Tel Model
114C floating differential dc amplifier operating at a gain of 50. The
output signal from the amplifier is fed into a type 3A1 dual trace

67

FIGURE 21.   VIEW OF HIGH SPEED SHUTTER AND SECONDARY MIRROR
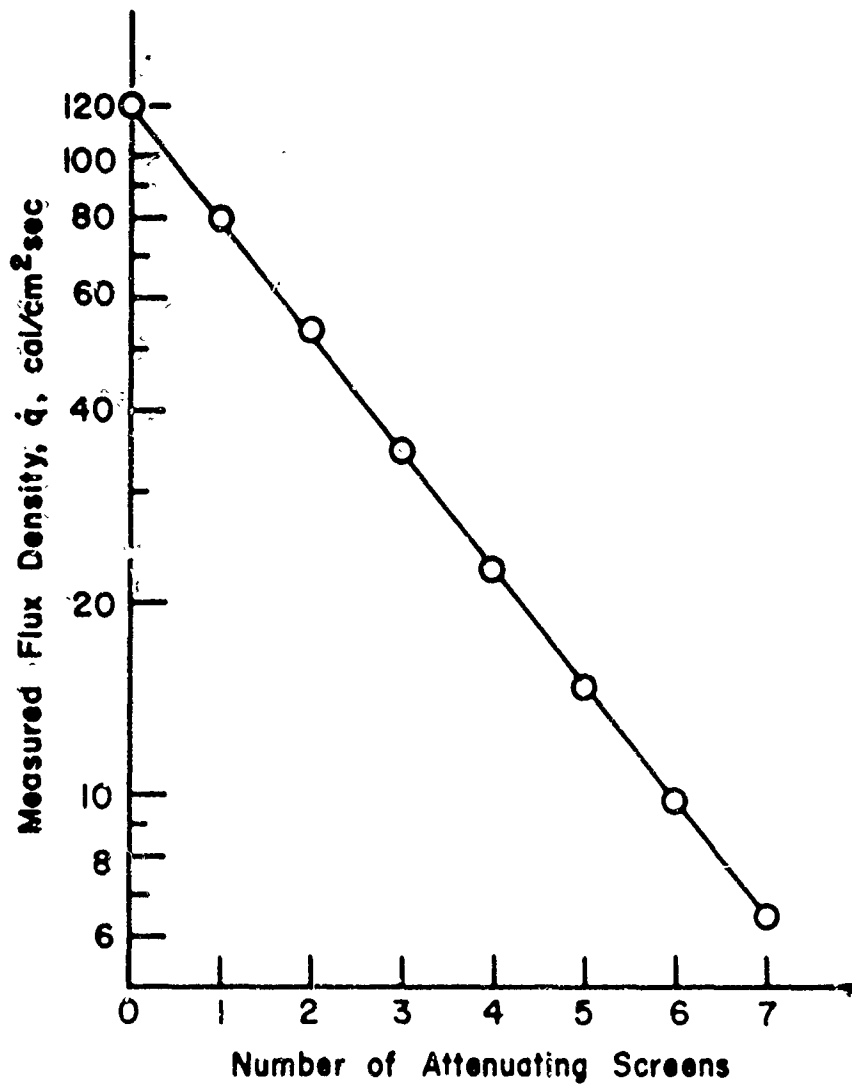WITH FLUX DENSITY ATTENUATING SCREEN IN POSITION.
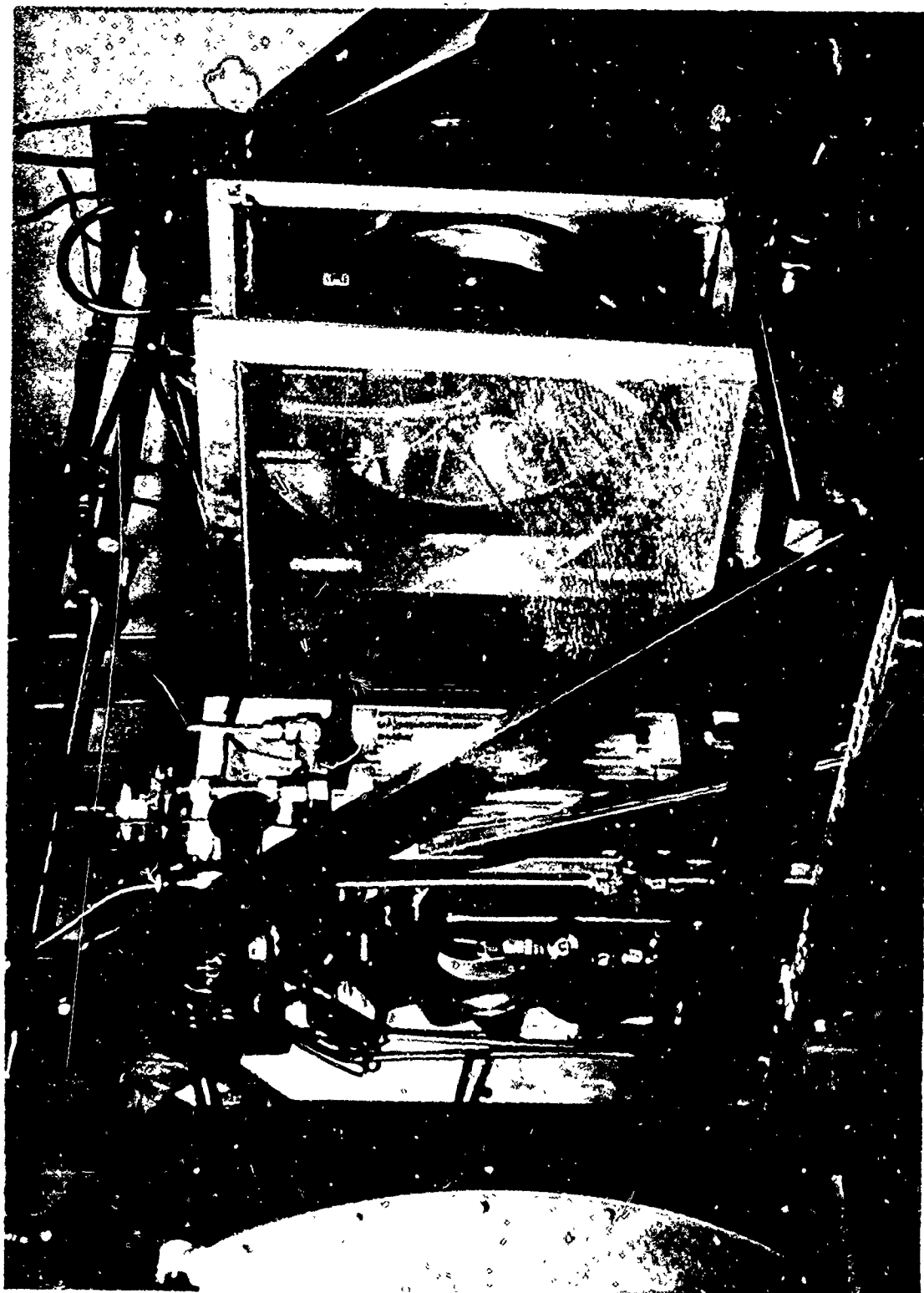
FIGURE 22. MEASURED FLUX DENSITY AS A FUNCTION OF THE
NUMBER OF LAYERS OF WIRE MESH SCREEN PLACED IN THE ENERGY
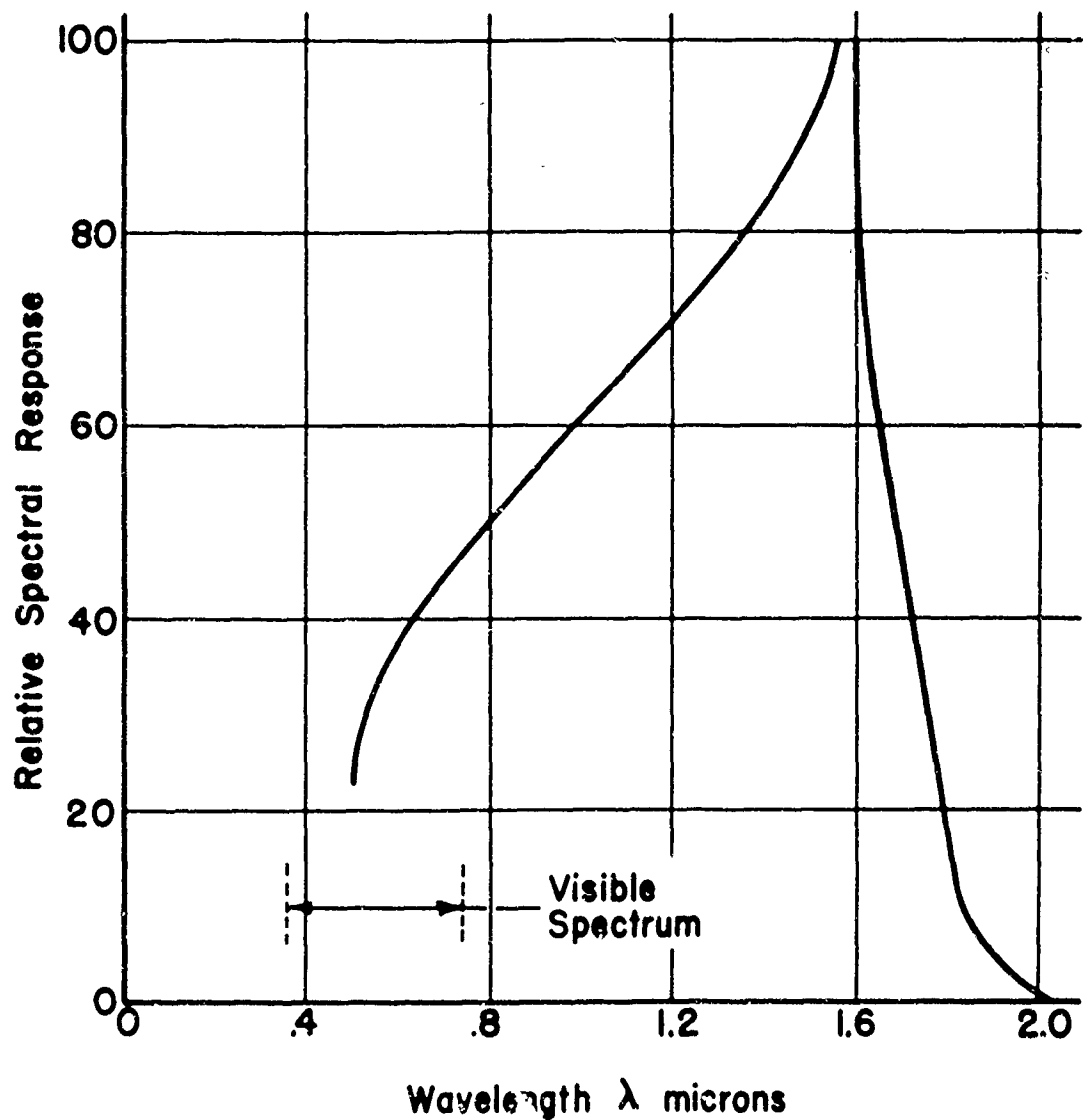BEAM. LAMP CURRENT CONSTANT AT 80 AMPS.

FIGURE 23. RELATIVE SPECTRAL SENSITIVITY OR RESPONSE
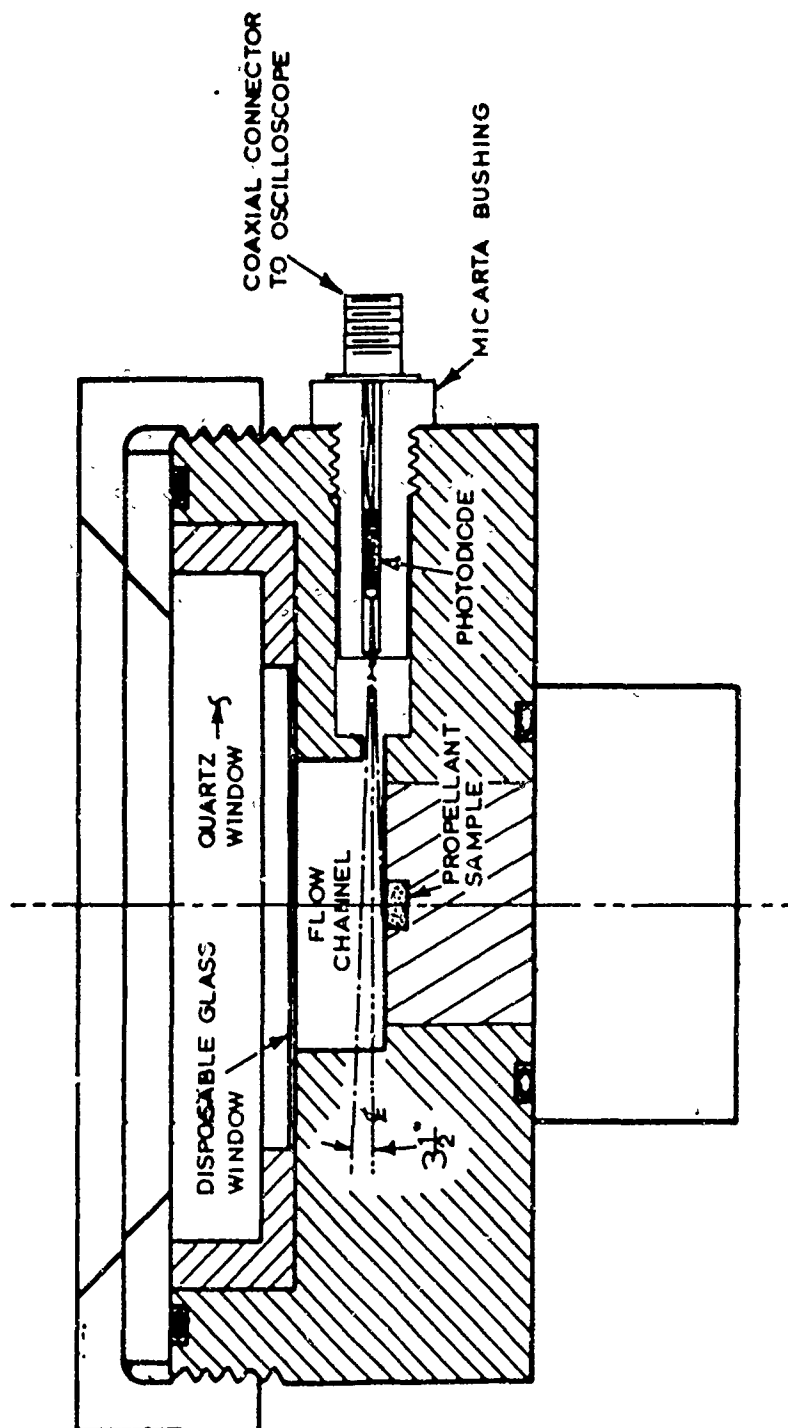OF THE GERMANIUM PHOTODIODE USED TO DETECT IGNITION.

FIGURE 24. CROSS SECTION OF IGNITION BOMB SHOWING
THE LOCATION AND LOOK ANGLE FOR PHOTODIODE.

amplifier in a 564 Tektronix storage oscilloscope. The entire signal
is floated above ground which has proven to be effective in preventing
pick-up of 60 cycle hum and other spurious signals.

In addition to sensing the self-luminosity of the reactions at
or near the surface of the sample, the photodiode also detects
scattered radiation from the sample holder surface and the opposite
wall of the flow channel. This scattered radiation is used to indicate
the opening of the shutter and hence the beginning of exposure time.
The oscilloscope trace is triggered by a 45 vdc pulse from a micro-
switch mounted on the shutter frame such that the switch is activated
just prior to the first perceptible shutter opening. Figure 25 shows
examples of ignition traces obtained in the present work.

The scattered radiation also acted as a disadvantage under the
general conditions of low pressure and high flux when tests were run
using inert gases. Here, the signal from luminous products is weak
(relative to high pressure self-luminosity) due to the lower concen-
tration. The scattered background radiation under these conditions is
strong and may in fact simply overwhelm the weak self-luminosity signal.
Under these conditions, it is usually possible to observe a radiation
signal of a strength comparable to steady state value, but it is not
possible to judge with any accuracy a precipitous onset of self-
luminosity. In the present work when either air or oxygen was used
as the environmental gas the sudden onset of self-luminosity was easily
detectable.

The possibility that a misinterpretation of the radiation trace
might result from a sudden increase in scattered radiation from the

FIGURE 25. IGNITION TRACES FOR A-87 PROPELLANT UNDER DIFFERENT
ENVIRONMENTAL CONDITIONS. LAMP CURRENT CONSTANT AT 77 AMPS, OS-
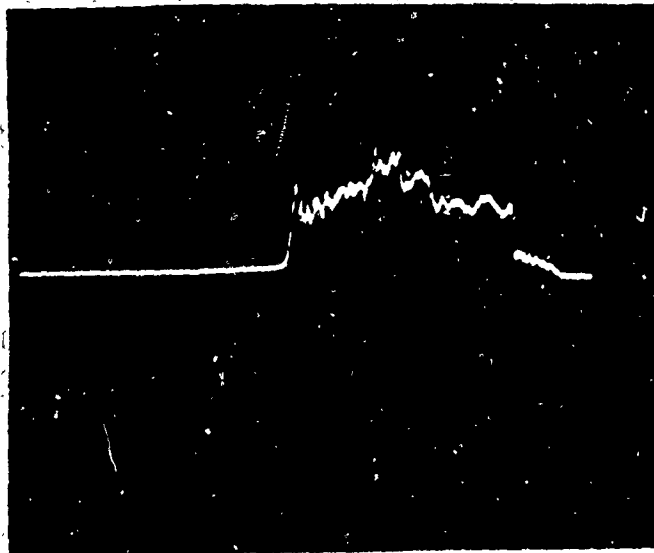CILLOSCOPE SENSITIVITY 0.01 V/CM, NO AUXILIARY AMPLIFIER USED.
(a) IGNITION IN 15 PSIA AIR, 6.12 CAL/CM^2 SEC, SWEEP 0.2 SEC/CM.
(b) IGNITION IN 100 PSIA AIR, 114 CAL/CM^2 SEC, SWEEP 0.005 SEC/CM.
(c) IGNITION IN 15 PSIA HELIUM, 6.12 CAL/CM^2 SEC, SWEEP 0.5 SEC/CM.
(d) IGNITION IN 100 PSIA OXYGEN, 114 CAL/CM^2 SEC, SWEEP 0.005 SEC/CM.
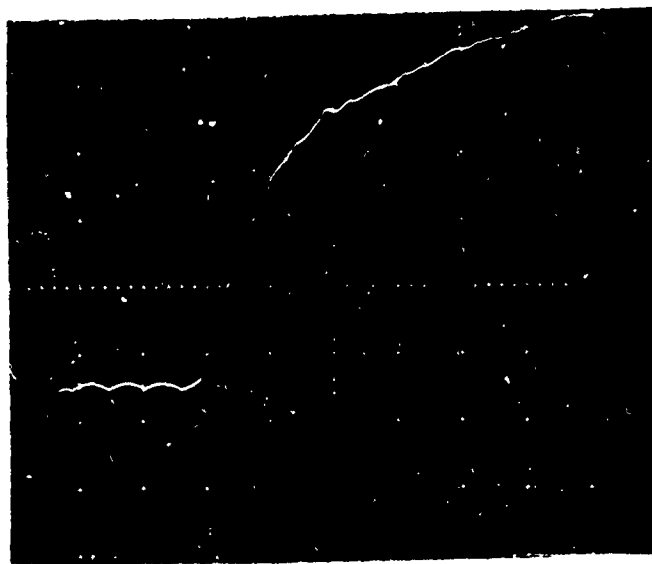
74
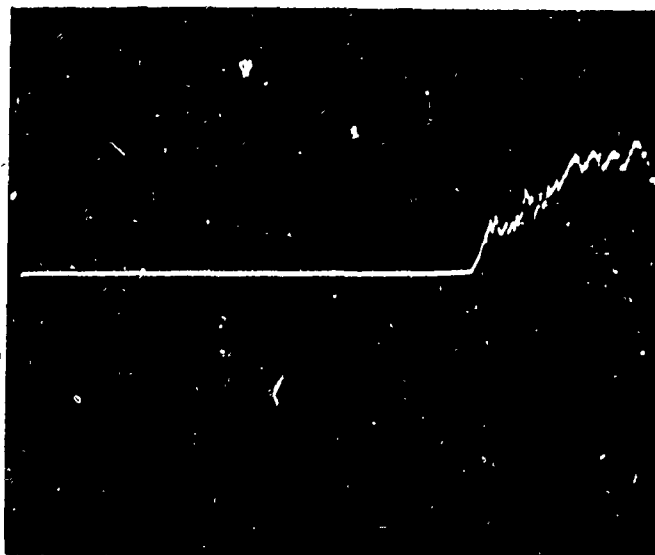
a. Ignition in 15 psia Air.
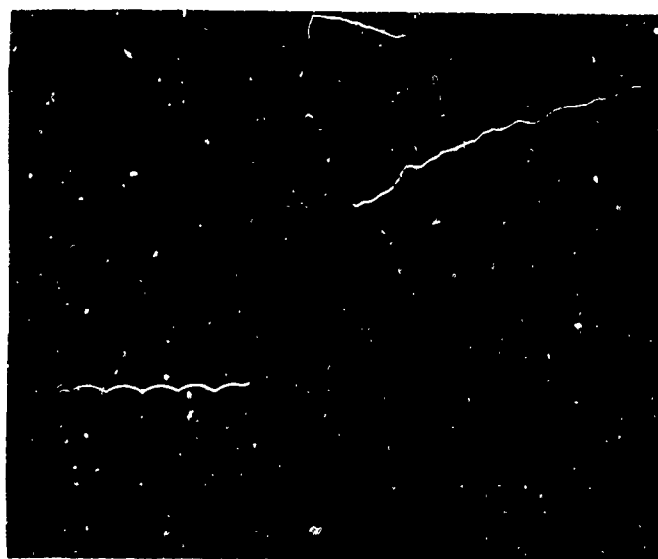
b. Ignition in 100 psia Air.
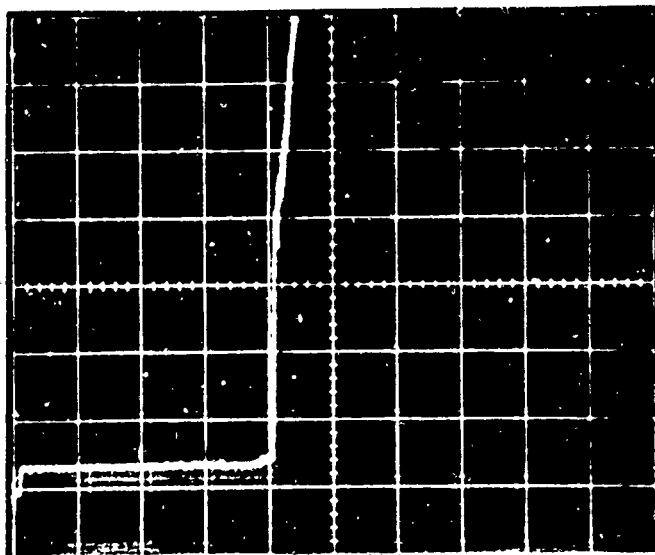
c. Ignition in 15 psia He.

d. Ignition in 100 psia O_2.

pyrolysis products of the propellant appearing in the gas phase as small particles or condensed droplets cannot be ignored. This was examined experimentally by running a "dummy" inert propellant in a nitrogen atmosphere and observing the level of scattered radiation due to decomposition products in the gas phase immediately above the propellant sample. A typical trace of this "inert radiation" is shown in Fig. 26b. A comparison of the level of radiation sensed by the photodiode in the inert case to the much higher level in the case of known ignition (the sample consumed itself) indicates that we are measuring the exposure time necessary to initiate strong exothermic reactions of a level that is of the order of magnitude associated with radiation from the propellant burning under steady state conditions. A comparison of the dummy propellant trace in nitrogen to the dummy propellant in oxygen is shown in Fig. 26.

SAMPLE EXPOSURE TIME

Ideally, the flux-time profile at the sample surface should be an instantaneous step function which would provide an unambiguous time base for the beginning of exposure time. It is not, of course, possible to achieve this in practice. In fact, only with some difficulty is it possible to realize 90 to 95 percent efficiency at the shortest exposure times. Since it is not possible to modulate the intensity of the source it is necessary to devise some type of mechanical shuttering. Here, the small cross-sectional area of the energy beam at the crossover point is utilized to good advantage. The small area offers the advantage of maximum operating speed without presenting insurmountable mechanical problems.

FIGURE 26. IGNITION AND PYROLYSIS FOR THE INERT DUMMY PROPELLANT. (a) DUMMY PROPELLANT IGNITION IN 100 PSIA OXYGEN AT 6.45 CAL/CM^2 SEC. SWEEP 0.5 SEC/CM, AMPLIFIER GAIN OF 50, OSCILLOSCOPE SENSITIVITY 0.1 V/CM. (b) DUMMY PROPELLANT PYROLYSIS IN 15 PSIA NITROGEN AT 9.8 CAL/CM SEC. SWEEP 0.2 SEC/CM, AMPLIFIER GAIN OF 50, OSCILLOSCOPE SENSITIVITY 0.2 V/CM.

a. Dummy Propellant Ignition
in 100 psia O_2.
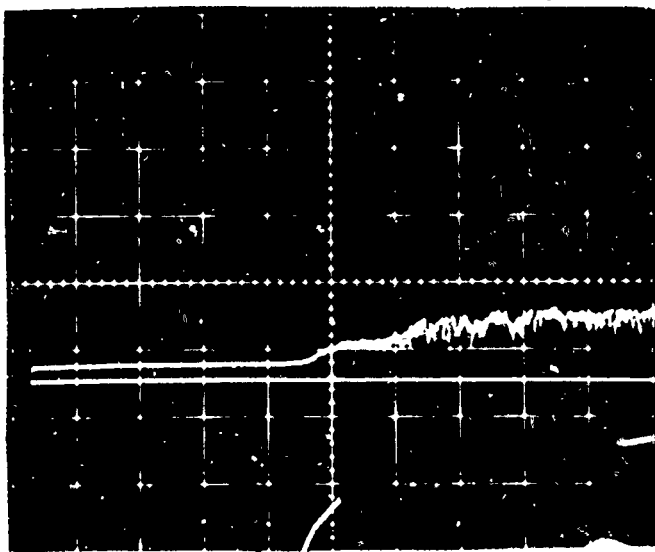
b. Dummy Propellant Decomposition
in 15 psia N_2.

The rapid exposure of the sample to the incident flux is controlled by a modified aerial camera shutter located at the crossover point. The shutter has a 3.5-inch diameter aperature with five iris-type stainless steel leaves. The original timing and actuation mechanisms have been replaced with a solid state electronic timer and switch to actuate a dc electric solenoid which releases a sear-catch allowing a powerful spring to open the shutter rapidly. A second identical shutter mechanism is mounted immediately behind the first shutter for an equally rapid termination of the exposure. The two-shutter system allows experiments to be run with precisely timed energy pulses. Such "controlled exposure time" experiments have not been made in the present investigation but are planned as a natural extension of this work. The thin leaves of the main shutter are protected from the relatively intense flux density at the crossover point by a 0.0625-inch thick stainless steel capping shutter that opens approximately 200 milliseconds before the main shutter opens. A heavy aluminum dowser on the lamp housing protects the entire shutter assembly during the time between tests. A microswitch mounted on the lamp house is actuated when the protective dowser is fully opened. This microswitch activates the electronic timer which opens the pneumatically powered capping shutter, rapidly followed by the main shutter. The shutter assembly is shown in Fig. 27.

The time required for the main shutter to fully open is approximately 2 milliseconds. The maximum flux density, however, was found to occur in approximately 1 millisecond from the start of opening over a diameter of 0.030 inches. This is a spot size somewhat smaller than

FIGURE 27. REAR VIEW OF HIGH SPEED SHUTTER WITH THE FIVE-BLADED
SHUTTER MECHANISM SHOWN IN THE OPEN POSITION. THE DC-SOLENOID-
SEAR COMBINATION USED TO ACTUATE THE SHUTTER MECHANISM CAN BE SEEN
ABOVE THE OPEN SHUTTER. BLOWER IN THE RIGHT FOREGROUND IS FOR
COOLING ATTENUATION SCREENS. TEST GAS FLOW METERS ARE SEEN MOUNTED
ON THE SHUTTER FRAME SIDE.
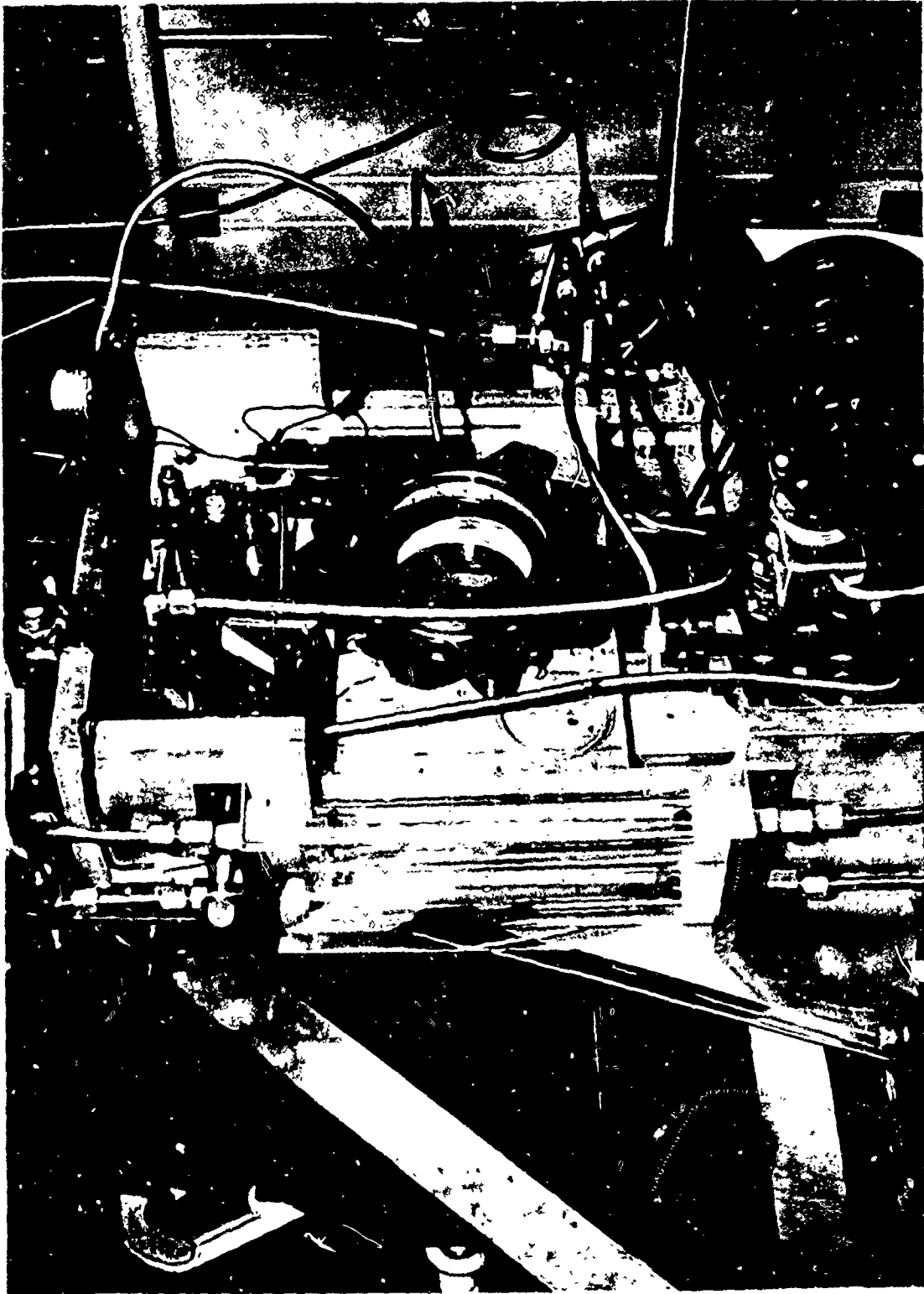
the final area defining the +5 percent of maximum flux. The maximum
flux density is formed at the sample surface before the energy beam
is fully traversed by the shutter blades because the shutter is located
at a focal plane. This is advantageous from the experimental stand-
point and the beginning of exposure time is taken as 1 millisecond from
the initial shutter opening trace.

SAMPLE COMPOSITION AND PREPARATION

The propellant selected for use in the present work is a typical
composite propellant designated as A-87 in the Aerothermochemistry
Division's experimental propellant series. A-87 is composed of 75
percent "as received" ammonium perchlorate, 23.5 percent PBAN (poly-
butadiene acrylic acid acrylonitrile terpolymer), 1.0 percent copper
chromite (Harshaw Chemical Cu 0202), and 0.5 percent carbon black.
The ammonium perchlorate particle size distribution is shown in Fig. 28.
The carbon black is a very fine powder with the particle size being
sub-micron. The copper chromite has a nominal particle size of 4
microns. The propellant ingredients were thoroughly mixed in a 15
pound batch in a vacuum and cured at 180°F for four days. The cured
propellant was machined into 8-inch long sticks with a 1-inch square
cross-section. These sticks were subsequently sliced in 0.25-inch
thick sections from which the cylindrical slugs were cut.

A dummy "inert" propellant was also formulated by replacing the
ammonium perchlorate with an equal volumetric loading of 50 micron
glass beads. The other constituants remained in the same proportion.
This inert mix was formulated and mixed by hand and cured in a small
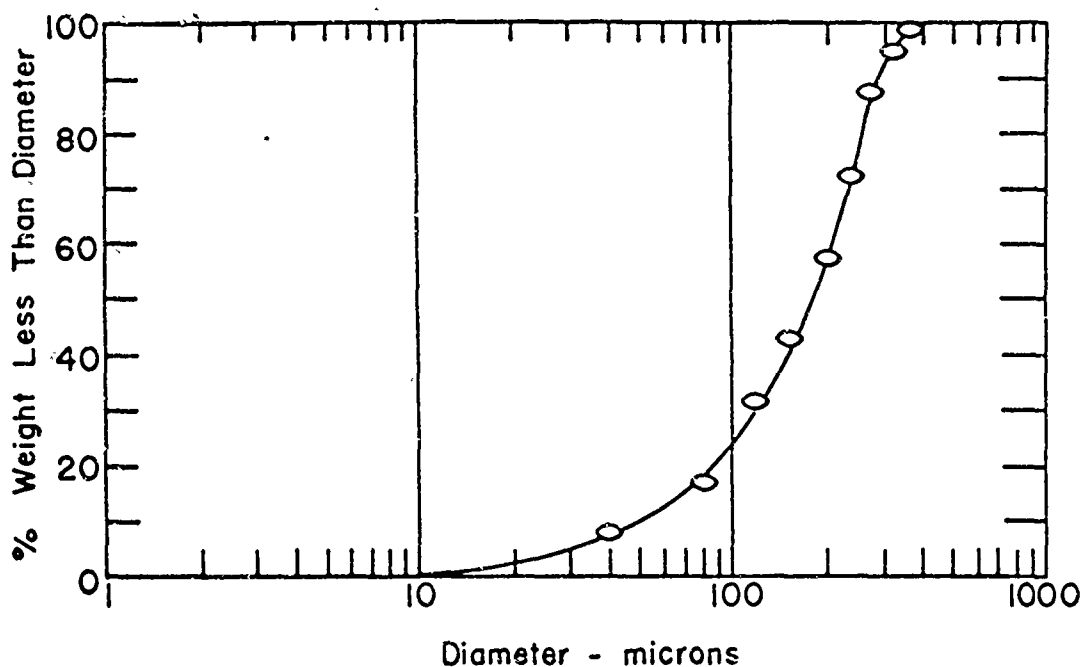vacuum oven. The cured batch contained numerous bubbles with the

FIGURE 28. PARTICLE SIZE DISTRIBUTION
FOR "AS RECEIVED" AMMONIUM PERCHLORATE.

result that only a small portion could be used. Attempts were made to use only sections that were free of bubbles.

Pressed pellets were formulated with 98 percent ammonium perchlorate, 1.3 percent copper chromite and 0.7 percent carbon black. These percentages represent the same weight ratios as the same ingredients in the propellant. The pellets were pressed at 40,000 psi and fit precisely in the sample holder.

ENVIRONMENTAL GAS SUPPLY AND FLOW METERING

With the exception of air all environmental gases used in the present work were supplied as bottled gases from the Matheson Company, Incorporated. Each bottle was mounted on a wall rack and equipped with a hand loaded regulator set for 150 psia. Figure 29 shows the gas

FIGURE 29. BOTTLED GAS STORAGE AREA.
NITROGEN BOTTLE AT LEFT IS USED TO
PURGE THE IGNITION BOMB WHEN NOXIOUS
GASES ARE USED.
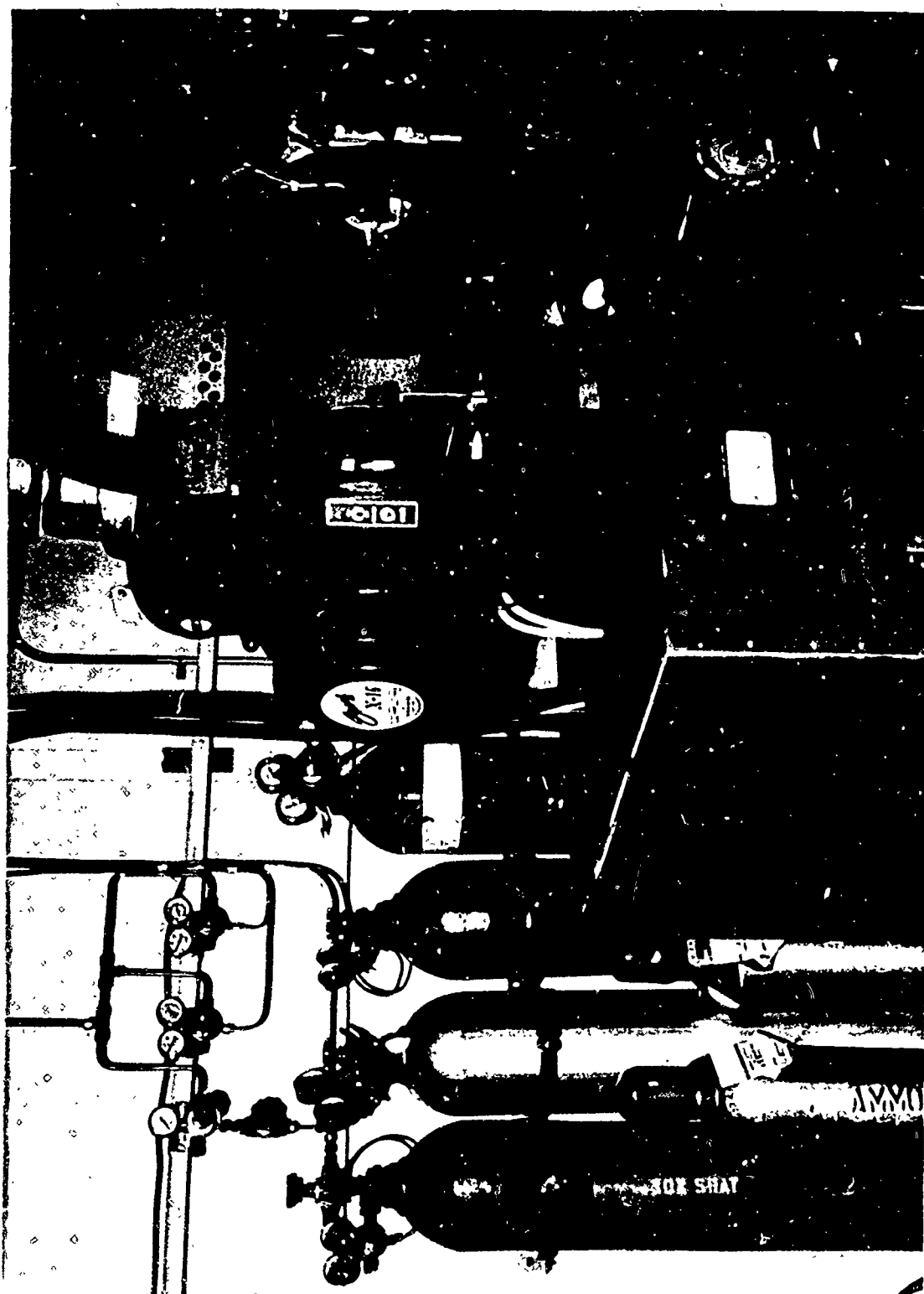
supply area with several bottles in the rack. The air was supplied dry
and filtered from the laboratory high pressure air facility. Each of
the gas regulators was connected to a common gas supply line with the
use of appropriate valving. The gas flow was metered before entering
the bottom of the ignition bomb by a standard number 5 Rodger Gilmont
rotameter. The meter reading was held constant for all runs. The
velocity past the sample surface then varied inversely with the square
root of bomb pressure. Flow velocities varied from 1 to 12 ft/sec
(see Appendix B).

The pressure in the bomb was varied with a hand valve in the
downstream exhaust line. Bomb pressure was monitored on a 0 to 300 psi
Heise gauge. The flowmeter reading was maintained constant while vary-
ing the bomb pressure by controlling the flow rate with a hand valve
located in the common gas supply line just upstream of the flowmeter.
The bottled gas was conserved by using a fast action toggle valve in
the common gas line. Once the flow rate and pressure was set by using
the control valves, it was found convenient to use the toggle valve for
turning the flow on and off just before and just after the particular
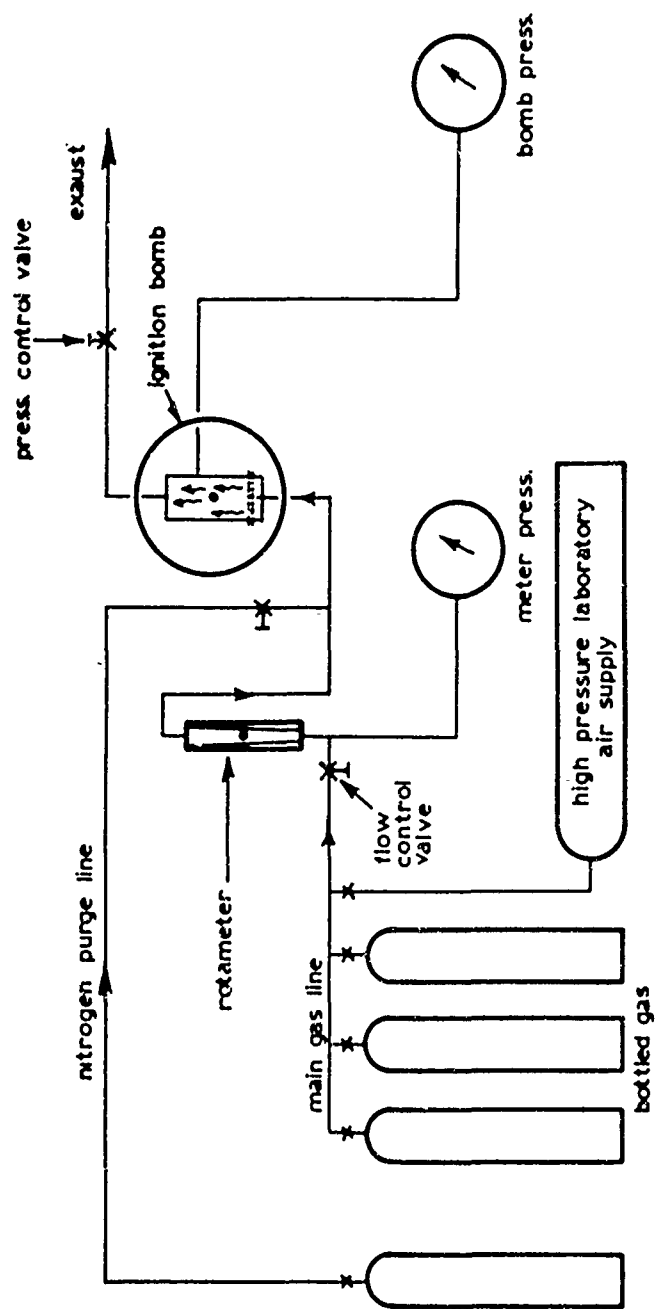test. Figure 30 is a sketch of the environmental gas flow system.

FIGURE 30. SCHEMATIC OF THE ENVIRONMENTAL GAS FLOW SYSTEM.

APPENDIX B

CHAMBER FLOW VELOCITIES

The flow of environmental gases into the ignition bomb was monitored by a No. 5 spherical float rotameter from the Rodger Gilmont Instruments, Inc. The generalized flow rate equation supplied with the meter is

$$\dot{Q} = 59.8 \ C_R \ R \left(\frac{R}{100} + 2 \right) \left(D_f \right) \left(\frac{W_f(\rho_f - \rho)}{\rho_f \ \rho} \right)^{\frac{1}{2}} \tag{1}$$

with $\dot{Q}$ in cc/min, C_R a dimensionless rotameter orifice coefficient, R a dimensionless diameter ratio, D_f the float diameter in inches, W_f the float weight in grams, and ρ_f and ρ the density gm/cc of the float and fluid flowing respectively.

The float density, ρ_f, is 2.53 gm/ml which is much greater than the gas densities, ρ, used and we may write with small error (less than 0.1 percent)

$$\dot{Q} = 59.8 \ C_R \ R \left(\frac{R}{100} + 2 \right) \left(D_f \right) \left(\frac{W_f}{\rho} \right)^{\frac{1}{2}} \tag{2}$$

A calibration chart was supplied with the meter for standard air and standard water. For all runs in the present work a constant meter scale reading of 30 was used. From the calibration chart the value of R was found to be 9. D_f is constant at 0.5 inches and W_f is constant at 2.715 gm. Then

89

$$\dot{Q} = 925 \ C_R \ 1/\rho^{\frac{1}{2}} \tag{3}$$

with ρ in gm/cc. Runs were made with air at standard conditions allow-
ing C_R to be calculated for those conditions. C_R for standard air is
0.89. Now $C_R = f \ (R^3/\mu^2)$ where μ is the absolute viscosity. For our
conditions R and temperature are constant so

$$C_R = \frac{C_R \ air \ \mu^2 \ air}{\mu^2}$$

and with μ^2 in $gm^2/cm^2 \ sec^2$, C_R for any gas is

$$C_R = \frac{3.045 \times 10^{-8}}{\mu^2}$$

Then from Equation (3) volumetric flow rates were found for all gases
tested. By the use of appropriate conversion factors and a knowledge
of the flow channel cross-sectional area, the environmental gas flow
velocities (average) past the sample surface were calculated. Table 1
lists the calculated values at static bomb pressures used.

Table 1

Gas	Velocity - ft/sec		
	15 psia	45 psia	100 psia
Air	3.23	1.86	1.25
Nitrogen	3.68	2.12	1.43
Oxygen	2.58	1.49	1.0
Methane	12.6	6.7	4.9
Helium	7.9	4.55	3.06

APPENDIX C

SURFACE HEAT TRANSFER COEFFICIENTS

In order to calculate surface heat transfer coefficients it is necessary to assume a flow model configuration. The flow channel is rectangular in cross section, 1.25 inches wide and 0.5 inches deep. Before entering the channel the gas passes through two porous stainless steel plates to distribute the flow evenly over the cross-section. The sample surface is located 1.25 inches from the last porous plate.

It was assumed that a reasonable model would be flow over a flat plate. Accordingly, the Reynolds number, Re, was checked to determine the flow region, i.e., laminar or turbulent. The transition was assumed to occur at Re $\leq$ 5 x 10^5. Under the present test conditions all flow was laminar with Re ranging from 8.35 x 10^2 for helium at 15 psia to 2.32 x 10^4 for methane at 100 psia. The characteristic length was taken to be 1.25 inches, the distance from the last porous plate to the sample location.

With flow in the laminar region the heat transfer coefficients were calculated from the following relationship [43]:

$$h_{cx} = 0.332 \frac{k}{x} Re^{\frac{1}{2}} Pr^{1/3}$$

The calculated values are tabulated in Table 2.

Table 2. Calculated Heat Transfer Coefficients

Gas	Pressure psia	h_{cx} BTU/hr ft^2°F	h_{cx} cal/cm^2 sec°C
Air	15	1.69	2.3×10^{-4}
	45	2.36	3.21
	100	2.72	3.7
Nitrogen	15	1.85	2.52
	45	2.42	3.3
	100	2.97	4.05
Oxygen	15	1.57	2.13
	45	2.04	2.77
	100	2.52	3.42
Methane	15	4.3	5.85
	45	5.45	7.4
	100	6.85	9.3
Helium	15	5.7	7.75
	45	7.5	10.2
	100	8.9	12.1

APPENDIX D

TABLES OF DATA

Table 3. Ignition Data for A-87
Time in Seconds and (seconds)$^{1/2}$

Cal/cm² sec	Air t	Air $t^{1/2}$	O₂ t	O₂ $t^{1/2}$	N₂ t	N₂ $t^{1/2}$	He t	He $t^{1/2}$	CH₄ t	CH₄ $t^{1/2}$	Pressure psia
6.45	1.25	1.118	1.253	1.12	1.27	1.126	1.96	1.40	1.48	1.22	15
	1.35	1.16	1.369	1.17	1.42	1.192	2.16	1.469	1.724	1.31	45
	1.48	1.215	1.59	1.26	1.62	1.273	2.65	1.628	1.96	1.40	100
9.8	0.648	0.805	0.63	0.794	0.69	0.83	0.88	0.938	0.712	0.844	15
	...	...	...	...	0.686	0.828	0.92	0.959	0.744	0.863	45
	0.682	0.826	...	...	0.784	0.885	1.072	1.035	0.933	0.966	100
15.0	0.352	0.593	0.329	0.574	0.361	0.601	0.410	0.64	0.361	0.601	15
	0.318	0.564	...	...	0.345	0.587	0.456	0.675	0.389	0.624	45
	0.335	0.579	0.352	0.593	...	...	0.498	0.706	0.423	0.653	100
22.5	0.20	0.447	0.172	0.415	0.207	0.455	0.240	0.49	0.212	0.460	15
	0.178	0.422	...	...	0.191	0.437	0.244	0.494	0.217	0.466	45
	0.180	0.424	0.166	0.407	0.173	0.416	0.265	0.515	0.212	0.461	100
34.5	0.120	0.345	0.0841	0.290	0.114	0.338	0.139	0.374	0.125	0.354	15
	0.094	0.31	0.0795	0.282	...	...	0.122	0.349	0.108	0.329	45
	0.082	0.286	0.0790	0.281	0.0896	0.299	0.129	0.360	0.114	0.338	100
52.5	0.082	0.286	0.0441	0.210	0.063	0.255	...	...	...	...	15
	0.053	0.23	0.0398	0.199	0.0572	0.239	0.066	0.257	0.073	0.270	45
	0.044	0.21	0.0384	0.196	0.0526	0.229	0.0714	0.267	0.0615	0.248	100
80.0	0.05	0.225	0.0241	0.155	...	...	...	...	...	...	15
	0.0324	0.18	0.022	0.148	0.0348	0.1865	0.0386	0.196	0.037	0.192	45
	0.026	0.162	0.0198	0.141	0.030	0.1732	0.0398	0.199	0.032	0.179	100
120.0	0.0404	0.201	0.0132	0.115	...	...	...	...	...	...	15
	0.023	0.15	0.0115	0.107	0.0198	0.1407	0.0236	0.152	0.025	0.158	45
	0.017	0.132	0.107	0.103	0.0164	0.1281	0.0232	0.152	0.0187	0.137	100

Table 4. Ignition Data of Dummy
Propellant in Oxygen at 100 psia

Time in Seconds and (Seconds)$^{1/2}$

Flux Density, $\dot{q}$, cal/cm^2 sec	Time t_i		Sq Rt Time $t_i^{1/2}$	
6.45	1.62	+0.38 / −0.39	1.273	+0.142 / −0.163
9.8	0.697	+0.20 / −0.132	0.835	+0.114 / −0.075
15.0	0.312	+0.079 / −0.047	0.559	+0.066 / −0.044
22.5	0.165	+0.035 / −0.024	0.406	+0.042 / −0.030
34.5	0.072	+0.012 / −0.012	0.268	+0.022 / −0.023
52.5	0.042	+0.004 / −0.007	0.206	+0.009 / −0.018
80.0	0.019	+0.007 / −0.005	0.138	+0.023 / −0.020
120.0	0.0127	+0.0003 / −0.0022	0.113	+0.001 / −0.011

Table 5. Ignition Data of Pressed
Pellets in Methane at 45 psia

Time in Seconds and $(Seconds)^{1/2}$

Flux Density, $\dot{q}$, cal/cm² sec	Time t_i	Sq Rt Time $t_i^{1/2}$
6.45	1.78	1.334
	1.88	1.370
	1.70	1.304
	1.55	1.245
	1.68	1.296
	1.65	1.284
9.8	0.935	0.997
	0.805	0.989
	0.760	0.97
15.0	0.410	0.640
	0.395	0.628
	0.445	0.668
22.5	0.200	0.447
	0.200	0.447
	0.200	0.447
34.5	0.088	0.297
	0.115	0.349
	0.123	0.350
52.5	0.055	0.235
	0.045	0.212
	0.051	0.226

DOCUMENT CONTROL DATA - R&D

(Security classification of title, body of abstract and indexing annotation must be entered when the overall report is classified)

1. ORIGINATING ACTIVITY (Corporate author)	2a. REPORT SECURITY CLASSIFICATION
Naval Weapons Center China Lake, California 93555	UNCLASSIFIED
	2b. GROUP None

3. REPORT TITLE

AN INVESTIGATION OF THE EFFECT OF ENVIRONMENTAL GASES AND PRESSURE ON THE IGNITION OF SOLID ROCKET PROPELLANTS

4. DESCRIPTIVE NOTES *(Type of report and inclusive dates)*

Research Report

5. AUTHOR(S) *(Last name, first name, initial)*

Hightower, J. D.

6. REPORT DATE	7a. TOTAL NO. OF PAGES	7b. NO. OF REFS
October 1967	100	72

8a. CONTRACT OR GRANT NO.	9a. ORIGINATOR'S REPORT NUMBER(S)
b. PROJECT NO.	NWC TP 4431
c. ORD-033 129/200 1/R001-06-01	9b. OTHER REPORT NO(S) (Any other numbers that may be assigned this report)
d.	

10. AVAILABILITY/LIMITATION NOTICES

This document has been approved for public release and sale; its distribution is unlimited.

11. SUPPLEMENTARY NOTES	12. SPONSORING MILITARY ACTIVITY
	Naval Ordnance Systems Command Department of the Navy Washington, D. C. 20360

13. ABSTRACT

An investigation was made of the effect of environmental gases and pressures on the ignition of an ammonium perchlorate propellant. In addition, ignition studies were conducted on the individual propellants ingredients. Environmental gases used were air, oxygen, nitrogen, methane and helium. Pressures were 15, 45, and 100 psia. Tests were run in oxygen on an inert mixture of the propellant binder and glass beads and on pressed ammonium perchlorate in methane. Ignition was initiated by radiant energy flux densities over the range of 6.5 to 120 cal/cm^2 sec in an arc-image furnace utilizing a 2,500 watt xenon source. The results indicate that the major exothermic reaction responsible for rapid convergence to steady state deflagration occurs in the gas phase immediately adjacent to the propellant surface.

The shortest ignition times were obtained with oxygen as the environmental gas. The ignition times of both propellant and inert formulation were the same in this environment. Ignition times of the propellant in nitrogen were longer than in oxygen but approximately the same as the ignition time of pressed pellets in methane. The ignition times of the propellant in inert atmosphere was found to increase with decreasing molecular weight of the environmental gas. At the higher flux densities the ignition time was found to be dependent on the environmental pressure with ignition times increasing with decreasing pressure. These results have been discussed in terms of a simple ignition model with (a) no chemical heating, (b) chemical heating in the condensed phase and (c) chemical heating in the gas phase.

DD FORM 1473 1 JAN 64   0101-807-6800

14. KEY WORDS	LINK A		LINK B		LINK C	
	ROLE	WT	ROLE	WT	ROLE	WT
Ignition						
Propellants						
Arc Image furnace						

INSTRUCTIONS

1. ORIGINATING ACTIVITY: Enter the name and address of the contractor, subcontractor, grantee, Department of Defense activity or other organization *(corporate author)* issuing the report.

2a. REPORT SECURITY CLASSIFICATION: Enter the overall security classification of the report. Indicate whether "Restricted Data" is included. Marking is to be in accordance with appropriate security regulations.

2b. GROUP: Automatic downgrading is specified in DoD Directive 5200.10 and Armed Forces Industrial Manual. Enter the group number. Also, when applicable, show that optional markings have been used for Group 3 and Group 4 as authorized.

3. REPORT TITLE: Enter the complete report title in all capital letters. Titles in all cases should be unclassified. If a meaningful title cannot be selected without classification, show title classification in all capitals in parenthesis immediately following the title.

4. DESCRIPTIVE NOTES: If appropriate, enter the type of report, e.g., interim, progress, summary, annual, or final. Give the inclusive dates when a specific reporting period is covered.

5. AUTHOR(S): Enter the name(s) of author(s) as shown on or in the report. Enter last name, first name, middle initial. If military, show rank and branch of service. The name of the principal author is an absolute minimum requirement.

6. REPORT DATE: Enter the date of the report as day, month, year; or month, year. If more than one date appears on the report, use date of publication.

7a. TOTAL NUMBER OF PAGES: The total page count should follow normal pagination procedures, i.e., enter the number of pages containing information.

7b. NUMBER OF REFERENCES: Enter the total number of references cited in the report.

8a. CONTRACT OR GRANT NUMBER: If appropriate, enter the applicable number of the contract or grant under which the report was written.

8b, 8c, & 8d. PROJECT NUMBER: Enter the appropriate military department identification, such as project number, subproject number, system numbers, task number, etc.

9a. ORIGINATOR'S REPORT NUMBER(S): Enter the official report number by which the document will be identified and controlled by the originating activity. This number must be unique to this report.

9b. OTHER REPORT NUMBER(S): If the report has been assigned any other report numbers *(either by the originator or by the sponsor)*, also enter this number(s).

10. AVAILABILITY/LIMITATION NOTICES: Enter any limitations on further dissemination of the report, other than those imposed by security classification, using standard statements such as:

(1) "Qualified requesters may obtain copies of this report from DDC."

(2) "Foreign announcement and dissemination of this report by DDC is not authorized."

(3) "U. S. Government agencies may obtain copies of this report directly from DDC. Other qualified DDC users shall request through
_____."

(4) "U. S. military agencies may obtain copies of this report directly from DDC. Other qualified users shall request through
_____."

(5) "All distribution of this report is controlled. Qualified DDC users shall request through
_____."

If the report has been furnished to the Office of Technical Services, Department of Commerce, for sale to the public, indicate this fact and enter the price, if known.

11. SUPPLEMENTARY NOTES: Use for additional explanatory notes.

12. SPONSORING MILITARY ACTIVITY: Enter the name of the departmental project office or laboratory sponsoring *(paying for)* the research and development. Include address.

13. ABSTRACT: Enter an abstract giving a brief and factual summary of the document indicative of the report, even though it may also appear elsewhere in the body of the technical report. If additional space is required, a continuation sheet shall be attached.

It is highly desirable that the abstract of classified reports be unclassified. Each paragraph of the abstract shall end with an indication of the military security classification of the information in the paragraph, represented as *(TS)*. *(S)*. *(C)* or *(U)*

There is no limitation on the length of the abstract. However, the suggested length is from 150 to 225 words.

14. KEY WORDS: Key words are technically meaningful terms or short phrases that characterize a report and may be used as index entries for cataloging the report. Key words must be selected so that no security classification is required. Identifiers, such as equipment model designation, trade name, military project code name, geographic location, may be used as key words but will be followed by an indication of technical context. The assignment of links, roles, and weights is optional.